CEAS Space Journal
https://doi.org/10.1007/s12567-024-00572-w

ORIGINAL PAPER

Comparative analyses of European horizontal-landing reusable first stage concepts

L. Bussler[1] · I. Dietlein[1] · M. Sippel[1]

Received: 5 April 2024 / Revised: 5 September 2024 / Accepted: 7 October 2024

Abstract
Partially reusable two-stage-to-orbit (TSTO) launch configurations have been investigated on system level by DLR in the ENTRAIN study which encompasses an examination of both vertical takeoff horizontal landing (VTHL) and vertical takeoff vertical landing (VTVL) reusable first stages. A target payload performance of 7.5 Mg into GTO is selected as the common mission requirement of all concepts. In this paper, the preliminary designs of TSTO configurations consisting of a winged reusable first stage and an expendable upper stage are presented and discussed. The considered propellant combinations include LOX/LH2, LOX/LCH4 and LOX/RP-1. Configurations based on staged combustion and gas generator cycle engines are analyzed. The focus of the presented preliminary analyses is on the overall performance of the space transportation system, the design and architecture of the winged reusable first stage and the comparison and evaluation of different VTHL configurations.

Keywords RLV · VTHL · Reusability · Space transportation systems

Abbreviations

AoA	Angle of attack
CAC	Calculation of aerodynamic coefficients
DOF	Degrees of freedom
ENTRAIN	European next reusable ariane
FB	Fly-Back
FPA	Flight path angle
GEO	Geostationary earth orbit
GG	Gas generator
GLOM	Gross lift-off mass
GTO	Geostationary transfer orbit
IAC	In-air-capturing
LCH4	Liquid methane
LH2	Liquid hydrogen
LOX	Liquid oxygen
RLV	Reusable launch vehicle
RP-1	Rocket propellant 1 (kerosene)
SC	Staged combustion
TSTO	Two-stage-to-orbit
US	Upper stage
VTHL	Vertical take-off horizontal landing

Nomenclature

Isp	Specific impulse [s]
L/D	Lift-to-drag ratio [-]
T/W	Thrust-to-weight ratio [-]
ΔV	Delta velocity [km/s]
ε	Expansion ratio [-]

1 Introduction

The presented work is part of a general, systematic analysis of RLV configurations in DLR, [1–5]. This investigation is motivated by an aspiration to identify suitable and advantageous concept designs for a future European reusable launch system. This sequence of papers deals with first stage reusability only, upper stage reusability is not considered. In any case, prior to any reuse the stage has to be recovered. This necessity poses the question of how to recover those parts of the space transportation system that shall be reused, which recovery strategy is promising and what are the technologies to be developed. For this purpose, DLR has committed a large system study comparing different two-stage-to-orbit (TSTO) concepts including both winged reusable first stages and non-winged reusable first stages landing vertically, see [1–5] for more details.

The focus of the present paper is on RLV systems with winged reusable first stages. Winged reusable first stages

✉ L. Bussler
Leonid.Bussler@dlr.de

[1] DLR Institute of Space Systems, Robert-Hooke-Straße 7, 28359 Bremen, Germany

Published online: 24 October 2024

landing horizontally need additional hardware in form of wings, empennage and landing gears and for some concepts air-breathing propulsion along with additional fuel. This increases the mass of the first stage and thus reduces the overall payload performance of the transportation system. However, several advantages as compared to vertical landing RLV stages exist. First, no additional rocket propellant for atmospheric reentry and a vertical landing of the stage needs to be foreseen in the design of the reusable stage. Furthermore, no additional rocket propellant needs to be accelerated during the ascent prior to being consumed along the descent trajectory. The wing allows a safe, non-propelled atmospheric reentry with controlled mechanic and thermal loads as well as a horizontal, aircraft-like landing on a runway. If air-breathing propulsion is installed on the winged reusable first stage, the operating radius of the stage is significantly increased with the achievable range depending on the aerodynamic and propulsion efficiency as well as the amount of air-breathing propulsion fuel. Two return options for winged reusable first stages are considered in this work: a fly-back (FB) booster-type stage returning to launch site by means of its own air-breathing propulsion and a stage returned to launch site through the IAC method.

The patented In-air-capturing (IAC) intends the winged reusable stages to be caught in the air and towed back to their launch site without any necessity of an own propulsion system. The idea has performance similarities with the vertical Down-Range Landing mode of VTVL stages. After decelerating to subsonics, the reusable stage is awaited by an adequately equipped capturing aircraft, offering sufficient thrust capability to tow a winged launcher stage with restrained lift-to-drag ratio. Significant progress in maturing the technology was reached in the Horizon 2020 project *FALCon* by performing sophisticated full-scale and lab-scale flight experiment simulations, [6]. A schematic illustration of the two different return options is shown in Fig. 1 (left FB, right IAC).

Numerous studies of reusable space transportation systems in and outside Europe have been performed in the past. The French space agency CNES studied two-stage configurations targeting 7.5 Mg to GTO, [7]. Amongst others, the analyzed systems were the Two-Stage-To-Orbit concept EVEREST and a semi-reusable concept RFS. In both cases, LOX/LH2 as propellant combination was used on the reusable stages. The reusable first stage (RFS) had a separation Mach number of around 13.5, while EVEREST was a Mach 6 separation concept. In [8] an overview of reusable systems with a focus on technology aspects of European programs is given. In addition, first stage reusability is considered to be a way to reduce launch cost. However, the need for further critical technology maturation is emphasized. One of the most detailed investigations in the area of winged, horizontally landing systems performed in the past in DLR in cooperation with German industry has been the ASTRA Liquid Fly-Back Booster (LFBB) study, [9]. The liquid boosters were meant as an option to replace the solid boosters of the Ariane 5 and relied on LOX/LH2 gas generator propulsion. Separation of the boosters was foreseen to take place around Mach 6 and air-breathing propulsion using H2 as fuel should have allowed a powered flight back to launch site. More recently, a reusable booster system has been studied in the U.S. and findings and recommendations concerning a number of technical, economical and operational aspects of RLV have been identified and formulated in [10]. A multidisciplinary approach is followed in [11]. In this work, winged RLV architectures are analyzed. While both glide-back and fly-back configurations are studied, finally the conclusion is drawn that the fly-back concept is a promising option. Within ESA's Future Launchers Preparatory Programme (FLPP), system studies to identify promising evolutions of the Ariane 6 launch vehicle towards a partially reusable launcher have been performed and are described in [12].

The content of the performed analysis presented in this paper is the technical assessment of partially reusable space

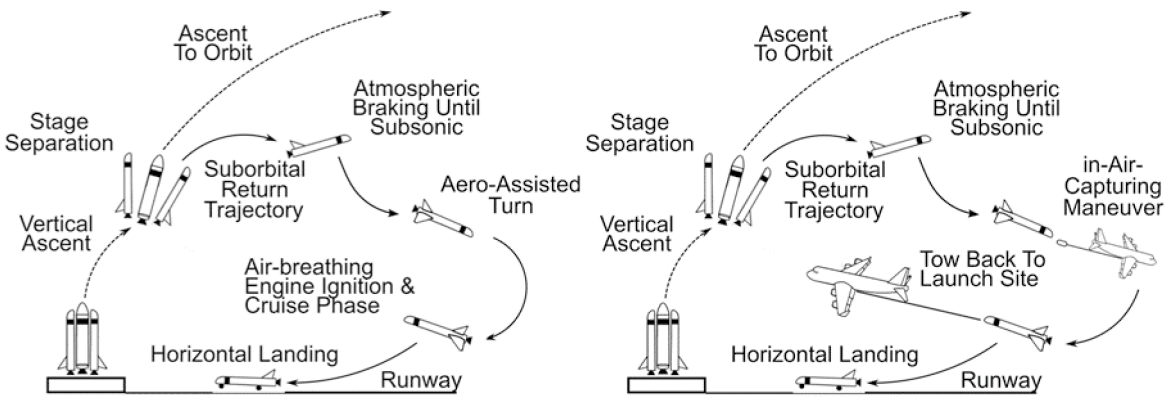

Fig.1 Return options for winged reusable first stages

transportation systems with winged reusable first stages. An important aspect of the work performed is to ensure comparability of the analyzed configurations by maintaining identical requirements w. r. t. launch site, target orbit, thrust-to-weight ratio (T/W) at launch, system architecture and payload mass, see also [1]. The ultimate objective is a contribution to the selection of feasible, promising and advantageous future European space transportation system concepts. The reference mission used for the predesign of various configurations consists of delivering 7.5 Mg to a geostationary transfer orbit (GTO) following a launch from Kourou. A unique feature of the presented work is its balanced compromise between the depth of the analysis for a specific configuration and the breadth of scope in terms of including different RLV stage return options, propellant combinations, engine cycles and staging velocities. Together with identical study requirements and assumptions, this compromise allows analyzing a greater number of potentially promising configurations on the one hand, and, on the other hand, performing a downselection based on sufficiently detailed calculations of all relevant aspects of a partially reusable space transportation system.

2 Description of study assumptions, requirements and methods applied

2.1 Study assumptions and general requirements

To identify the different configurations without ambiguity, a specific nomenclature is used. This configuration nomenclature specifies the type of fuel (RP1 = kerosene, C = methane, H = hydrogen), the rocket engine cycle (GG = gas generator, SC = staged combustion), the reusable first stage separation velocity class (Hi = high separation velocity, Med = medium separation velocity, Lo = low separation velocity) and the specific first stage return method (IAC = In-Air-Capturing, FB = fly-back). More details can be found in [1].

The following space transportation configurations with winged reusable first stages landing horizontally are analyzed and presented in this paper:

- Winged reusable first stages with fly-back capability (FB):
  - LH2/LOX SC with 6.6, 7.0 and 7.6 km/s upper stage ΔV
- Winged reusable first stages without fly-back capability, needing to perform either a down-range landing or rely on additional means as In-Air-Capturing (IAC):
  - LH2/LOX SC with 6.6, 7.0 and 7.6 km/s upper stage ΔV
  - LH2/LOX GG with 7.0 km/s upper stage ΔV
  - LCH4/LOX GG with 7.0 km/s upper stage ΔV
  - RP-1/LOX GG with 7.0 km/s upper stage ΔV

Parameters that are considered important to obtain comparable reusable first stages are: thrust-to-weight ratio (T/W) at launch and upper stage delta velocity (ΔV). A T/W of 1.4 is fixed for all configurations. Upper stage nominal ΔVs of 6.6, 7.0 and 7.6 km/s are considered for hydrogen staged combustion VTHL configurations. An upper stage ΔV of 7.0 km/s is used for all remaining configurations. The above ΔV values refer to nominal changes in velocity during powered flight, ΔV losses due to gravity, atmospheric drag and thrust orientation are not included. The upper stage ΔV is chosen to define the staging point of the launcher. Given a certain total mission velocity increment, the upper stage ΔV as well defines the ΔV of the reusable first stage. However, the upper stages are all classical, expendable rocket stages and hence using the ΔV of these conceptually similar systems is obvious. Details concerning the selection of upper stage ΔVs are given in [1].

The propellant combinations under investigation are LOX/LH2, LOX/LCH4 and LOX/RP-1. The liquid rocket engine propellant feed cycles considered are the staged combustion (SC) and gas generator (GG) cycles. Another important aspect is the assumption of the same fuel/oxidizer combination for the reusable first stages and the expendable upper stages. Also, the same type of engine with different expansion ratios ε is used for the lower and upper stages. The number of stages is set to two for all analyzed configurations regardless of the propellant combination. Tandem staging is used for all configurations. First and upper-stage diameters are identical. The propellant tanks of the reusable first stage as well as the expendable upper stage share a common bulkhead.

The principal study assumptions are summarized below:

- Reference mission: delivery of 7500 ± 150 kg to GTO
- Two stage, tandem staging configurations
- T/W of 1.4 at launch
- Geostationary Transfer Orbit (GTO) parameters: 250 km × 35,786 km, 6° inclination
- Launch site: Kourou, French Guyana, 52.77° W / 5.24° N

For RLV stages a system mass margin of 14% is applied to all components except the propulsion subsystem. For expendable upper stages a margin of 10% is applied to all components except the propulsion subsystem. For components of the propulsion subsystem, a margin of 12% is applied for both RLV and expendable stages. Propellant reserves of 0.9% relative to the ascent propellant mass are foreseen for all fuel/oxidizer combinations. In addition, a propellant reserve of 25% is foreseen for the subsonic cruise

flight towards the launch site for winged fly-back boosters. The amount of fly-back propellant reserve is oriented upon the ASTRA LFBB configuration, see [9].

It should be noted that performance-wise winged reusable first stages without fly-back capability are equivalent to configurations landing down range of the launch site. From an RLV stage performance point of view no additional hardware and/or fuel for a flight back to the launch site are foreseen in the design of these stages. Furthermore, no consideration of any operations to bring the stages back to the launch site is performed within this study. In the following, the In-Air-Capturing method is the assumed method for return to the launch site of these RLV stages without fly-back capability.

2.2 Mass modelling and structural analysis

For the mass model definition, a combination of empirical methods and preliminary structural analysis based on selected load cases and structural concepts is used. The empirical mass estimation methods are based on stage loads and masses as well as geometrical parameters of the respective component. For the structural analysis, beam theory and methods for stiffened shells are used. Load cases considered for structural analysis have been limited to ascent load cases. Masses of major structural elements as tanks, inter stage structures and thrust frames are obtained by structural analysis. An example of a structural analysis result is shown in Fig. 2. Apart from the visualization of the entire system structure (except for the wing and empennage) a close view on one of the tanks including the chosen stringer and frame geometries (not to scale) is shown. Empirical methods are applied for the majority of the remaining elements of the mass models. In particular, the VTHL first stages wing mass is determined with empirical methods. Dimensioning parameters are lateral acceleration, stage dry mass as well as wing area, span and maximum thickness of the wing (root airfoil section).

The following ascent load cases are considered for the structural analysis:

- Maximum dynamic pressure
- Maximum product of dynamic pressure and AoA
- Maximum acceleration
- Launch pad in presence of wind loads, launcher full and pressurized
- Pad release

Tanks are modelled as stringer-frame stiffened common bulkhead tanks from aluminum alloy AA2219. Tank pressures are between 3 and 4 bars. Aerodynamic forces are computed with empirical methods. Wing forces are introduced as discrete forces acting at several points along the wing root chord. A safety factor of 1.25 is applied.

2.3 Trajectory simulation and optimization

The ascent and descent trajectories are calculated using the DLR in-house tool TOSCA (Trajectory Optimization and Simulation of Conventional and Advanced Space Transportation Systems), [13]. This tool allows the calculation of ascent and descent trajectories flown by launchers, spacecraft and reentry vehicles through the solution of the equations of motion of a point mass (3 DoF). The atmospheric

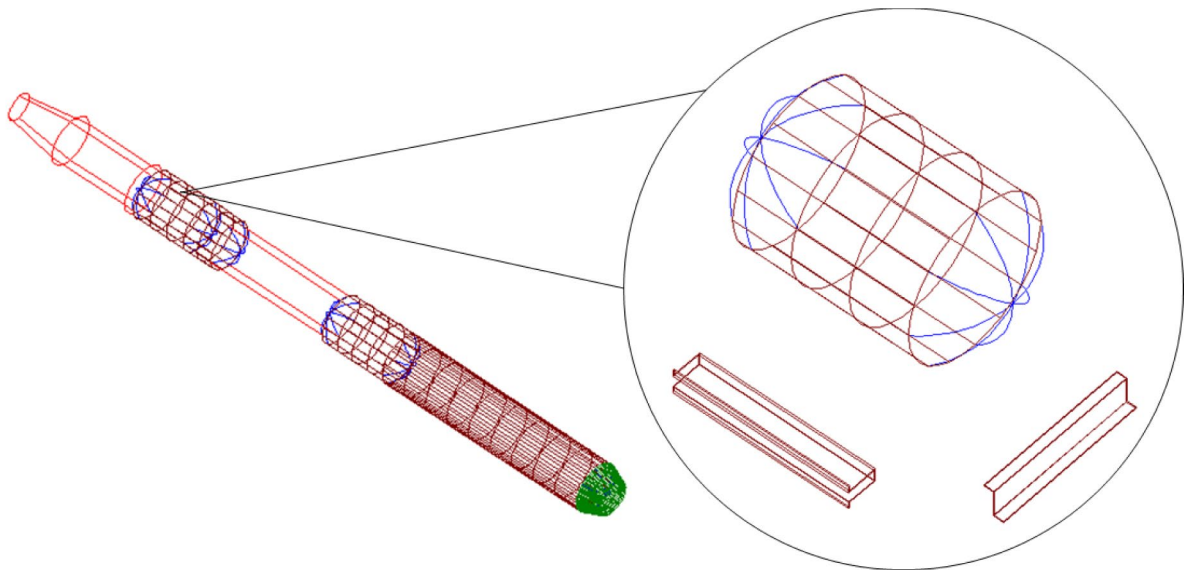

Fig. 2 An example of RLV first and ELV upper stage structural design

model used is oriented on the NRLMSISE00 model for Kourou, [14]. In all simulations, no wind is considered.

Ascent trajectory optimization is performed with a direct method and is based on Sequential Quadratic Programming (SQP). The payload mass delivered to orbit is the optimization objective while pitch rate, thrust angle (w. r. t. velocity), bank angle and thrust throttling are possible control variables. Furthermore, additional constraints can be defined. For the present study pitch rate and thrust angle are used as controls. Axial acceleration is in general limited to 50 m/s^2. Rocket engines are throttled upon reaching this boundary. It is important to note that due to the requirement that the line of apsides of the GTO ellipse has to be in the equatorial plane, upper stage (US) flight is split into two thrust phases with a ballistic phase in between, see Fig. 3. The initial part of the ascent thus consists of the first stage thrust phase followed by the first thrust phase of the upper stage and allows reaching an intermediate orbit that is followed until crossing the equator. There, the upper stage is reignited and apogee reaches GEO altitude. Only the first part of the ascent towards the intermediate orbit is optimized, the second thrust phase of the upper stage is simulated. For most of the configurations the intermediate orbit has a perigee altitude of around 140 km, an apogee altitude of around 330 km and an inclination of 5.9°. Second phase upper stage delta velocity is approximately 2.4 km/s. The ascent trajectory of the VTHL reusable first stage concepts is on the one hand optimized with the objective of maximum payload to target orbit, on the other hand, the trajectory is constrained considering the peak thermal loads during atmospheric reentry of the reusable stage. In particular, it is attempted to lower the flight path angle at separation by increasing the pitch rate as long as dynamic pressure at separation is below 1 kPa and upper stage thrust angle (w. r. t. velocity) is able to balance out the higher pitch rate. This approach results in small losses of payload mass but significantly reduces the thermal loads during the subsequent reentry phase.

No reentry trajectory optimization is performed for the VTHL reusable first stages. The reentry trajectories are iteratively simulated. Control of normal acceleration is achieved by variation of angle of attack. A limit of 4 g is set for the normal acceleration. Bank angle is varied to initiate a turn and achieve the desired heading towards the launch site.

Following the atmospheric reentry and turn, air-breathing engines are used for a powered return to launch site in case of the fly-back configurations. The amount of fuel required for the subsonic return flight depends on the stage mass, the distance to be travelled, the efficiency of the air-breathing propulsion system, the aerodynamic performance of the fly-back booster in the subsonic regime as well as the flight Mach number and altitude. Initially, the return cruise flight using air-breathing propulsion was simulated with a 4 DoF approach to determine the fly-back fuel mass, see [15]. Currently, a simplified approach using the Breguet equation with average values of aerodynamic and propulsion efficiency coming from the detailed simulations is used to calculate

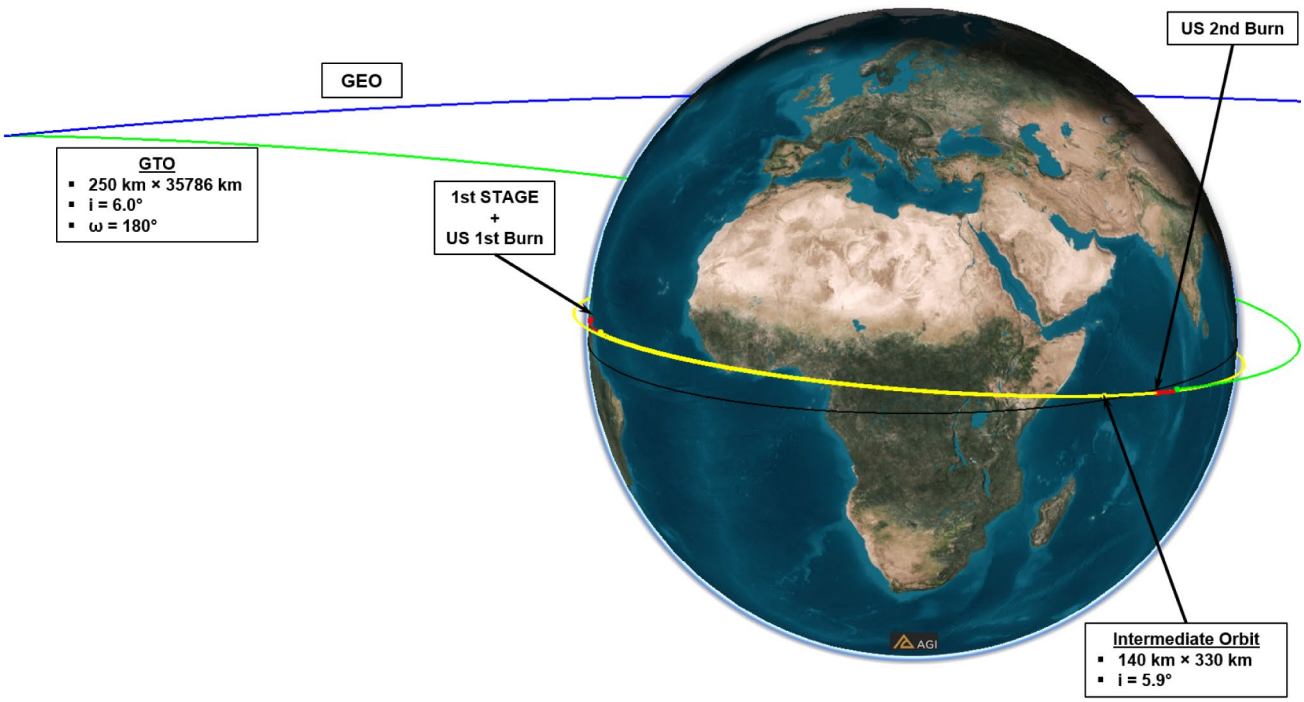

Fig. 3 Strategy followed for the ascent of the VTHL configurations

the fly-back fuel mass. For the in-air-capturing, the capture and tow-back are not simulated as this portion has, apart from the hardware to be installed on the returning stage, no impact on the launcher performance. The aforementioned hardware is considered within the mass budget.

2.4 Modelling of aerodynamics, aerothermodynamics and thermal protection system

Aerodynamic forces and moments are modelled with DLR in-house tools CAC (Calculation of Aerodynamic Coefficients) and HOTSOSE (Hot Second Order Shock Expansion). These programs allow the fast calculation of aerodynamic coefficient maps required for trajectory simulations depending on the angle of attack, Mach number and altitude or Reynolds number. CAC is used for ascent aerodynamics and the sub- and supersonic regimes of the reentry. HOTSOSE is used in the hypersonic regime of the reentry.

CAC is based on empirical and analytical methods and follows a superposition approach for obtaining total aerodynamic coefficients for a certain geometry. The methods implemented can be based on relationships from potential theory such as e. g. lifting-line theory for wing lift calculation as well as empirical relationships resulting from experimental work. More information on the theoretical background and the methods applied within the CAC program can be found in [16] and [17].

HOTSOSE is a tool for hypersonic aerodynamics and aerothermodynamics. The implemented aerodynamical methods are based on inviscid surface inclination methods applicable in hypersonic flow. Within the tool, e.g. the modified Newtonian method and the second-order shock expansion method are used. Besides modelling air as an ideal gas, the consideration of high-temperature effects in HOTSOSE is possible. Functions for the thermodynamic and transport properties are implemented for chemically reacting air in equilibrium. Apart from aerodynamic coefficients as functions of angle of attack and Mach number, temperature and heat flux distributions can be obtained. Surface temperature is user-specified or calculated based on the assumption of radiation adiabatic equilibrium. An exemplary surface temperature distribution is shown in Fig. 4. More details can be found in [18].

The Thermal Protection System (TPS) is a crucial component for VTHL configurations. In the frame of the current study, the mass of the thermal protection system is estimated based on the selected TPS materials and the thermal loads experienced during atmospheric reentry. The VTHL first stages discussed in this work employ TPS materials such as Space Shuttle-type Flexible Reusable Surface Insulation (FRSI), Tailorable Advanced Blanket Insulation (TABI) and Alumina Enhanced Thermal Barrier (AETB) ceramic tiles as well as ceramic matrix composites (CMC) for highly loaded

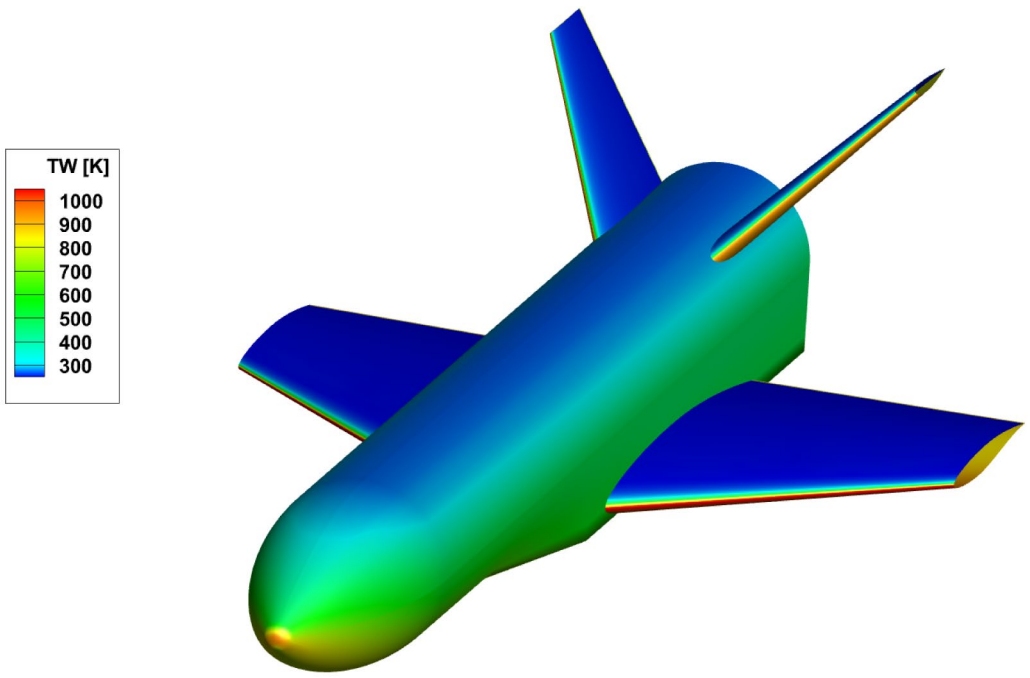

Fig. 4 Example of HOTSOSE results in the form of equilibrium temperature distribution – first stage of H SC Lo IAC configuration (altitude = 47 km, AoA = 46 deg, Ma = 5.9)

areas. A more detailed description of these materials can be found in [19]. The external thermal loads are determined with the tool HOTSOSE. Following the determination of the external loads and the definition of a maximum acceptable temperature limit beneath the thermal protection, the TPS thickness and mass are iteratively calculated assuming one-dimensional heat transfer. Radiation adiabatic equilibrium is assumed for the outer wall.

2.5 Propulsion and propellant supply system

To ensure comparability of the designed launchers, generic engines with identical baseline assumptions are needed for the systematic assessment and comparison of future RLV stages. The selected technical characteristics of these generic engines are oriented towards data of existing types as well as previous or ongoing development projects, [3]. The two rocket engine cycles most commonly used in first or booster stages are included in the study:

- Gas-Generator cycle (GG)
- Staged-Combustion cycle (SC)

The main combustion chamber (MCC) pressure is commonly set to 12 MPa for the gas-generator type. This pressure is not far from the useful upper limit of this cycle but is assumed necessary to achieve sufficient performance for the RLV stages, [3]. In the case of staged combustion engines, the MCC pressure is fixed at 16 MPa. This moderate value has been chosen considering the limited European experience in closed-cycle high-pressure engines, [3]. Nozzle expansion ratios in the first stage are selected according to optimum performance. Expansion ratio is set to 35 for both gas generator and staged combustion engines. The upper-stage engines are derived from the first stage engines with the only difference being the expansion ratio. Its value is set to 120 as a reasonable first assumption and considering inter-stage structure length requirements.

All preliminary engine definitions have been performed by simulation of steady-state operation at 100% nominal thrust level using the DLR tools LRP (Liquid Rocket Propulsion) and NCC (Nozzle Contour Calculation) as well as the commercial tool RPA (Rocket Propulsion Analysis). Any potential requirements specific to transient operations are not considered in this early design study. Turbine entry temperature (TET) is set around 750 K and kept in all cases below 800 K to be compatible with the increased lifetime requirement of reusable rocket engines, [3]. Further, all engines considered in this study are designed with regeneratively cooled combustion chambers and regenerative or dump-cooling of the downstream nozzle extensions. Table 1 presents the mixture ratio (MR), the sea level (SL) and vacuum (Vac.) specific impulse (Isp) for the first and upper stage rocket engines considered within the study. More details on the performed rocket propulsion analysis can be found in [3].

The propellant supply system including feedlines, fill/drainlines and the pressurization system was modelled using the DLR in-house tool PMP. This program is able to calculate the respective masses for these systems by calculating the propellant and pressurizing gas flow throughout the whole mission and thus sizing the required hardware. Autogenous pressurization is assumed for all configurations except the LOX/RP-1 systems. Here the RP-1 tanks are pressurized with helium. The tool also calculates the mass of the cryogenic insulation of the tanks. It is important to note that insulation was only considered a necessity in the case of LOX/LH2 launchers due to the low temperature of LH2. In the case of hydrocarbon launchers, no insulation is used since it adds mass and it is assumed that it is technically feasible to fly cryogenic propellants without insulation (e. g. Falcon 9 with LOX/RP-1). This assumption is to be verified by a thermal analysis beyond the scope of this study.

In the case of FB as a reusable first stage return-mode, air-breathing engines are used for the return cruise flight. Their efficiency, i.e. their specific fuel consumption or specific impulse, is important not only from an RLV, but also from an overall configuration design point of view. The specific impulse of air-breathing engines depends on the type of fuel and is one of the main drivers for fly-back fuel mass. While kerosene would be a classic choice its specific impulse is in the area of 4000 s, whereas hydrogen potentially offers a specific impulse of more than 10000 s for typical turbofan engines at subsonic Mach numbers.

Thus, the selected air-breathing engines for FB configurations within this study are modified EJ200 of MTU Aero Engines without afterburner that can be operated with

Table 1 First and upper stage rocket engine data, [3]

Propellants	*First Stage*				*Upper Stage*			
	LOX/RP-1	*LOX/LCH4*	*LOX/LH2*		*LOX/RP-1*	*LOX/LCH4*	*LOX/LH2*	
Cycle	GG	GG	GG	SC	GG	GG	GG	SC
MR [-]	2.25	2.5	6	6	2.25	2.5	6	6
SL Isp [s]	267	276	351	385	–	–	–	–
Vac. Isp [s]	320	331	418	438	338	349	440	459

hydrogen after minor modifications, see [20]. Furthermore, they have a high specific thrust and thrust-to-weight ratio. Thrust and specific fuel consumption characteristics of EJ200 have been calculated with DLR in-house air-breathing propulsion tool. The calculated installed thrust characteristics as a function of altitude for subsonic Mach numbers from 0 to 0.8 is shown in Fig. 5. A summary of calculated EJ200 characteristics is given in Table 2.

Table 2 EJ200 calculated installed characteristics for operation with H2 at return flight conditions

Ma [-]	Altitude [km]	Thrust [kN]	sfc [g/kN s]	Isp [s]
0.3	4.0	35	9.01	11,300
0.4	5.0	32	9.30	11,000
0.5	6.0	29	9.57	10,700
0.6	7.0	26	9.78	10,400
0.7	8.0	23	9.91	10,300

3 Preliminary design of VTHL configurations

In this section, the preliminary design of the VTHL configurations as well as specific aspects of winged reusable first stage design are discussed. All analyzed configurations are two-stage systems and use tandem staging. A selection of configurations with a nominal upper stage delta velocity of 7.0 km/s is shown in Fig. 6.

The following structural segments are considered within the mass model and/or structural analysis for all analyzed configurations (top to bottom): payload fairing, upper stage fuel tank, upper stage oxidizer tank, upper stage thrust frame, interstage structure, lower stage oxidizer tank, lower stage fuel tank, lower stage wing, lower stage thrust frame, rear skirt. The length of the interstage structure is influenced by the length of the upper stage engine and the first stage nose structure. First stage nose structure length is set to 7 m for all configurations. Upper stage engine expansion ratio is fixed to $\varepsilon = 120$ for all studied variants, [3]. However, depending on the choice of propellant combination and first stage separation velocity and thus the efficiency as well as the thrust requirement for the upper stage engine, its nozzle size can differ substantially. Stage diameters are between 5.0 and 6.0 m and overall configuration height is between 70 and 83 m.

3.1 Winged reusable first stage architecture

The general layout of a VTHL reusable first stage is shown in Fig. 7 exemplified by the H SC Med IAC stage. The LOX tank is shown in blue, while the LH2 tank is shown in red. All analyzed VTHL first stages are equipped with a single delta wing and a V-tail. The single delta wing uses an RAE 2822 airfoil and has a leading-edge sweep angle of 40 degrees. The chord lengths of the main wing and V-tail are functions of the stage length. Identical ratios of chord length to overall stage length are used for all configurations. From the point of view of pure subsonic aerodynamic performance, a straight wing with a high aspect ratio would be

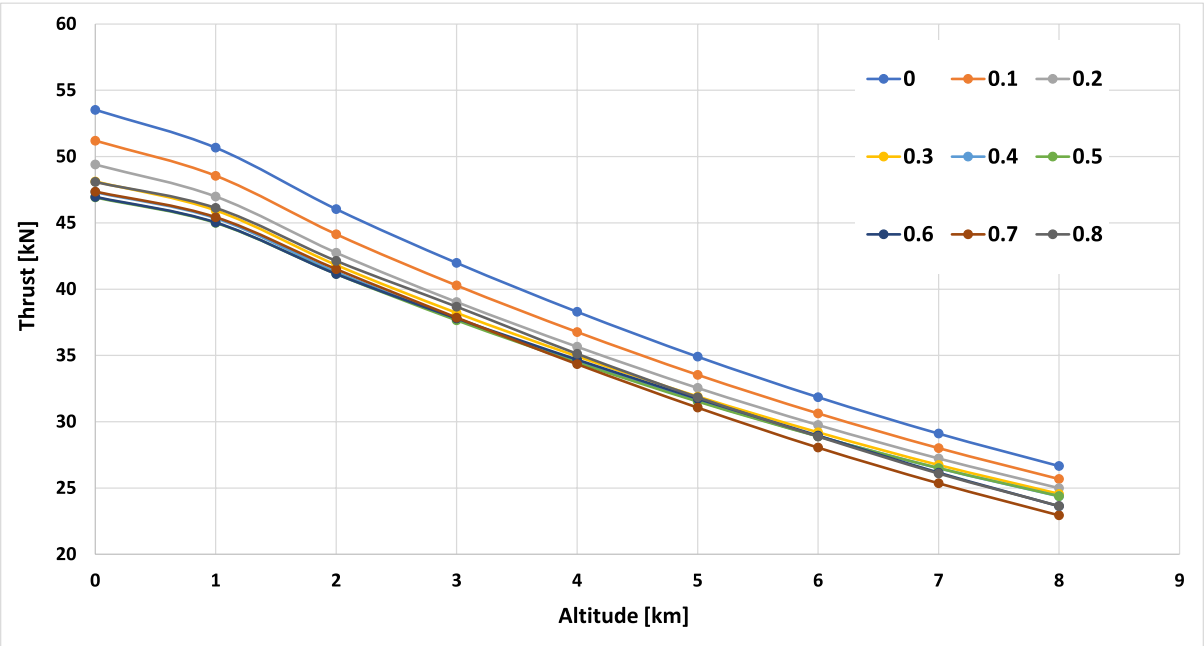

Fig. 5 Calculated installed thrust characteristics of EJ200 turbofan

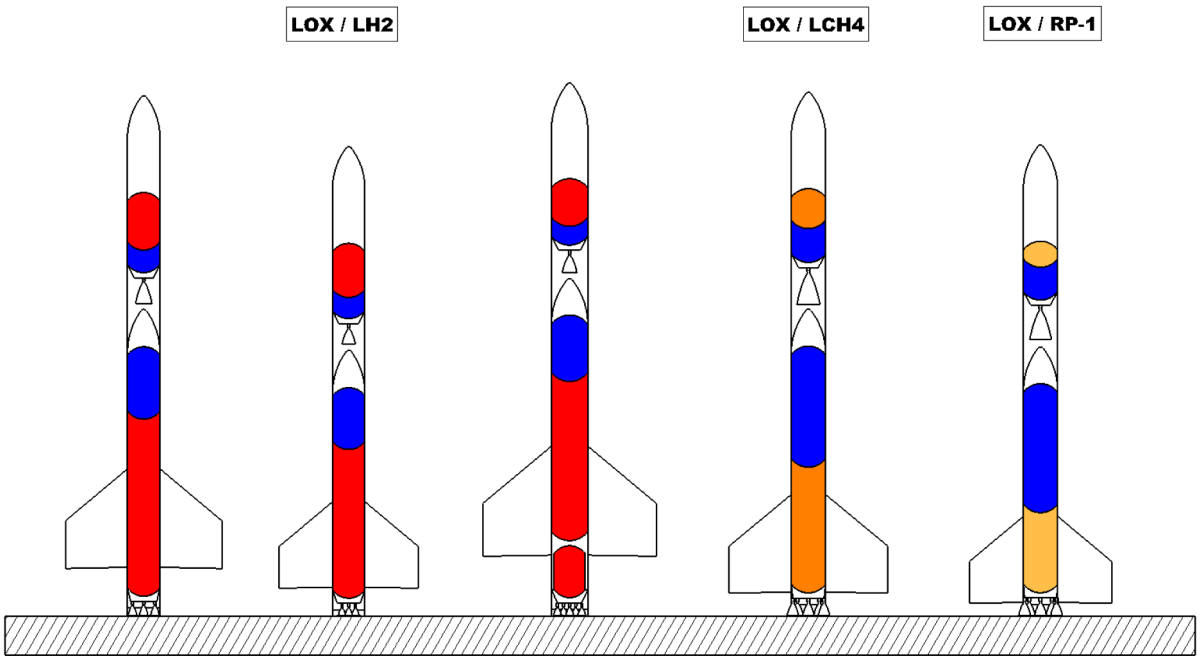

Fig. 6 VTHL configurations with 7.0 km/s upper stage delta velocity, LOX = blue, LH2 = red

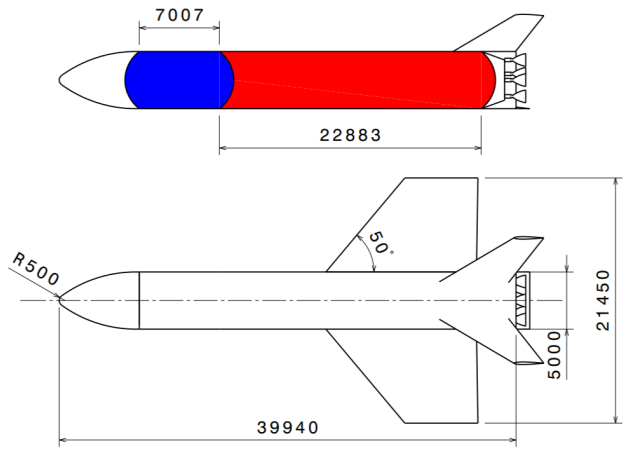

Fig. 7 H SC Med IAC VTHL reusable first stage, LOX = blue, LH2 = red (unit of length: mm)

advantageous. However, this is not realistic for an RLV stage with a fixed wing. The analyzed single delta wing fly-back stages have L/D ratios between 5 and 6 at subsonic Mach numbers. Typical trimmed lift-to-drag ratios of the analyzed VTHL winged reusable first stages are shown in Fig. 8 for subsonic, supersonic and hypersonic Mach numbers.

Several aspects have an influence on the stage diameter: the dimensions of the payload to be transported, the accommodation of first stage rocket engines and the desired length-to-diameter ratio of the first stage. The first two aspects are setting lower limits for the stage diameter. For VTHL configurations a length-to-diameter ratio of 9 is considered desirable for the winged reusable first stage for aerodynamic stability and trimmability reasons. A body flap and wing flaps are used for aerodynamic control. The body flap is used exclusively in the hypersonic regime and is deflected only downward. The minimum stage diameter considered for the presented VTHL configurations is 5.0 m. The nose segment radius is 0.5 m for all analyzed configurations. In the case of FB as return mode, air-breathing engines are located in the nose segment (see box in Fig. 9) and an additional non-integral fly back fuel tank is placed behind the main, integral LH2 tank, see Fig. 9. Between four and six air-breathing engines are used on FB stages.

3.2 Design iteration loop

This subchapter presents the design iteration loop followed by the iterative preliminary analysis. Independent of the VTHL return option, the analysis iteration is initiated with a design that is based on an initial guess and experience with similar or comparable configurations. Propulsion data, a mass model and an aerodynamics model allow a first ascent trajectory simulation and optimization. This is the case for either of the two considered return options, namely fly-back (FB) and In-Air-Capturing (IAC). Flow charts for both of the analyzed VTHL return options are shown in Fig. 10 and Fig. 11.

After the first ascent trajectory calculation, the performance in the defined target orbit is assessed. In case the payload

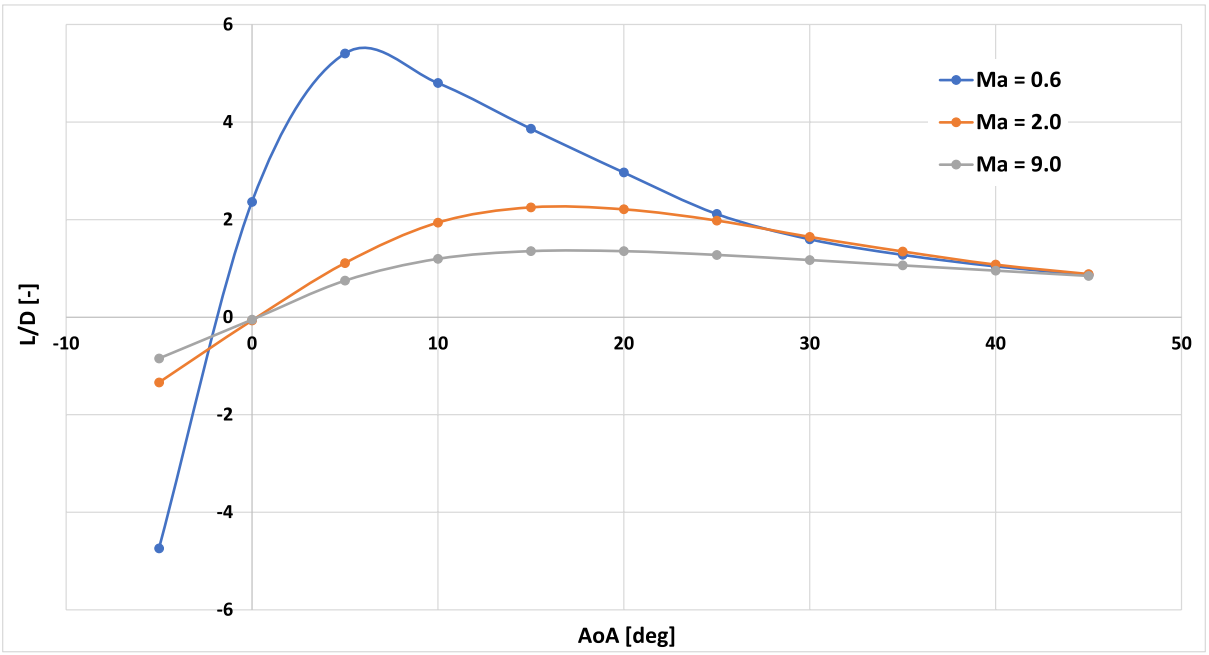

Fig. 8 Trimmed lift-to-drag ratios of winged RLV stages

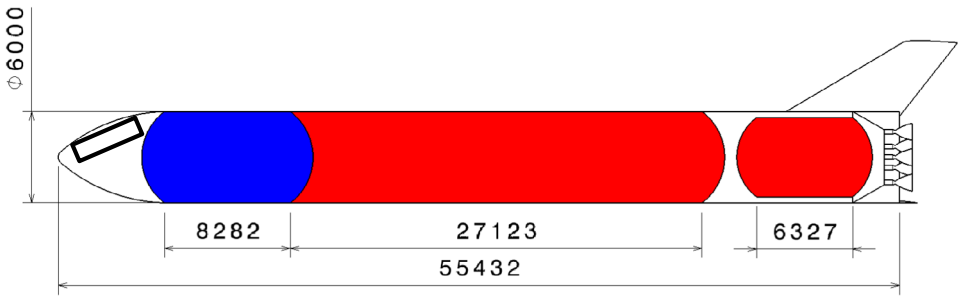

Fig. 9 H SC Hi FB VTHL reusable first stage, LOX = blue, LH2 = red

target is not met, a reiteration of the ascent performance is done until the resulting payload mass, the overall configuration and also the particular stages are compliant with the defined requirements. The necessary adaptations can include changing the ascent propellant masses, the rocket engine thrust as well as the geometry of the configuration. Once the payload performance is within the defined boundaries, a calculation of the winged reusable first stage descent trajectory can be performed. The state at separation of the first stage defines the initial conditions of the descent calculation. Depending on the particular reentry trajectory and the associated aerothermal loads, the thermal protections system (TPS) mass is determined and compared with the current value in the mass model. Convergence is reached when no substantial difference exists between the thermal protection system mass calculation based on the latest reentry trajectory and the TPS defined in the previous step of the mass model. In contrast to the IAC configurations whose design iteration loop includes ascent and atmospheric reentry calculations only, in the case of FB the return cruise flight back to the launch site with air-breathing engines is as well calculated and part of the iteration, see Fig. 11. This means that depending on the distance to the launch site after performing the atmospheric reentry and turn, the stage mass, the specific impulse of the air-breathing engines as well as the trimmed subsonic lift-to-drag ratio a fly-back fuel mass is calculated that is again input to the mass model and the entire design iteration loop is continued until convergence is achieved, see Fig. 11.

4 Results

4.1 Overview on investigated configurations

In this work, nine VTHL configurations are analyzed. A data summary of the nine converged VTHL configurations

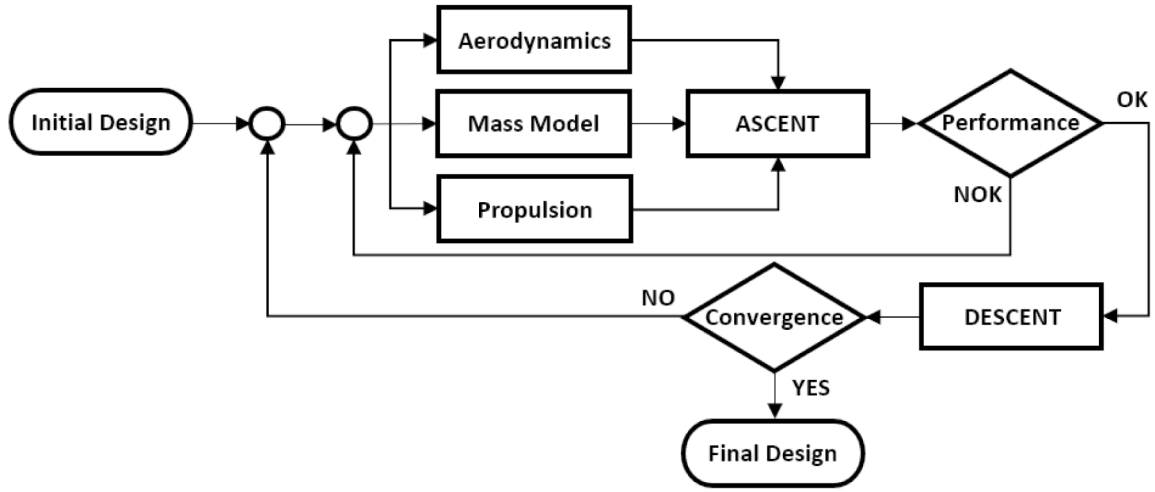

Fig. 10 Design iteration loop for IAC systems

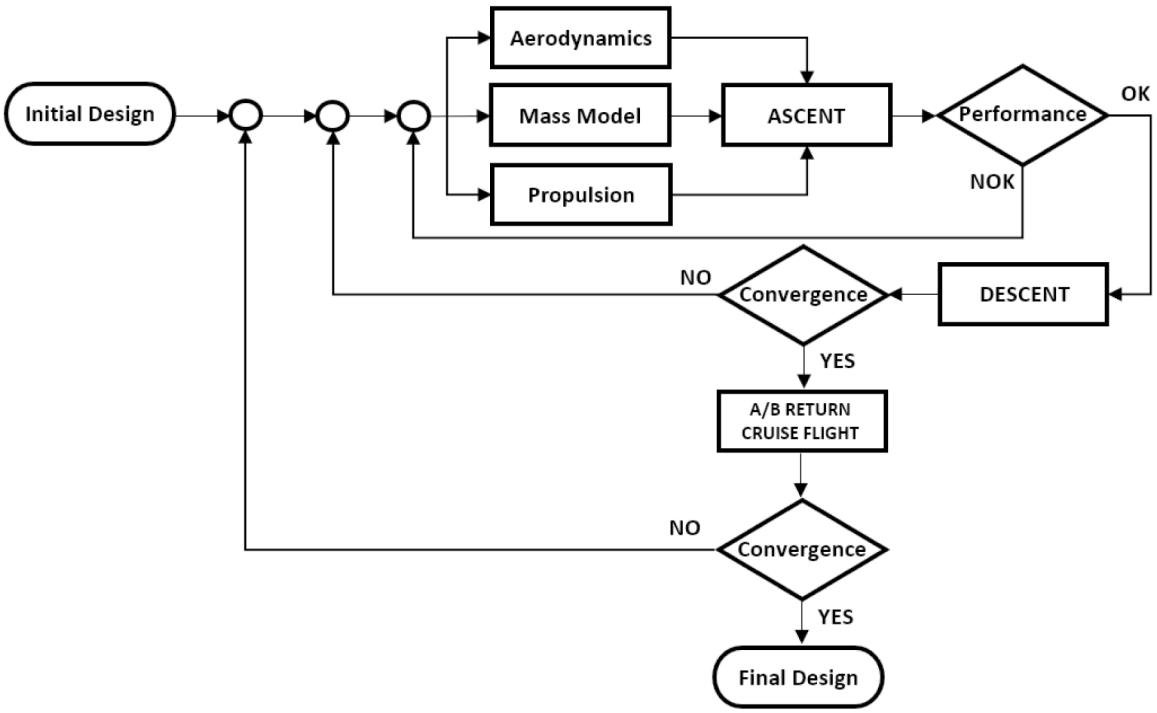

Fig. 11 Design iteration loop for FB systems

is given in Table 3. Six out of them are relying on staged-combustion rocket engines, the remaining ones are using gas-generator engines. One configuration each uses LOX/LCH4 and LOX/RP-1 as propellant combination, the remaining ones are LOX/LH2 designs. For all designs the same propellant combination is used on the RLV and the expendable upper stage, hybrid configurations are not investigated. Gross lift-off masses (GLOM) span a range from approximately 330 Mg to 870 Mg, the corresponding payload fractions are between 0.9% and 2.3%.

Table 3 Summary of investigated VTHL configurations

		LH2 SC			LH2 SC			LH2 GG	LCH4	RP-1
Return Option		FB	FB	FB	IAC	IAC	IAC	IAC	IAC	IAC
Engine Cycle	–	SC	SC	SC	SC	SC	SC	GG	GG	GG
2nd stage Δv	[km/s]	6.6	7.0	7.6	6.6	7.0	7.6	7.0	7.0	7.0
First Stage Separation Velocity Class	–	Hi	Med	Lo	Hi	Med	Lo	Med	Med	Med
Winged Reusable First Stage										
Ascent Propellant	[Mg]	350	275	230	225	205	190	245	575	635
Total dry mass	[Mg]	83.0	66.3	55.7	40.1	35.4	33.8	45.3	53.2	49.5
Propulsion mass	[Mg]	20.9	17.4	14.8	8.6	8.1	8.0	7.7	15.1	14.9
No. of engines	[-]	9	7	5	7	6	5	7	9	9
Single Engine Thrust (sea level)	[kN]	814	870	1098	681	757	908	766	1246	1323
Expendable Upper Stage										
Ascent Propellant	[Mg]	57.5	68.1	83.4	56.4	64.6	83.2	73.3	150.0	150.4
Total dry mass	[Mg]	6.1	6.3	7.2	5.4	5.8	6.8	6.0	7.7	7.5
Propulsion mass	[Mg]	1.7	1.8	2.2	1.4	1.6	1.9	1.4	2.3	2.3
Engine Thrust (vacuum)	[kN]	967	1035	1304	810	900	1080	961	1574	1674
Launcher Configuration										
Height	[m]	82.7	80.5	80.9	72.4	70.8	71.7	78.9	78.3	70.2
Diameter	[m]	6.0	5.6	5.2	5.0	5.0	5.0	5.0	5.3	5.3
Payload to GTO	[Mg]	7.59	7.52	7.41	7.46	7.59	7.46	7.38	7.43	7.58
GLOM	[Mg]	528.9	442.4	400.8	344.4	328.8	332.5	389.3	814.5	870.9
P/L Fraction	[%]	1.4	1.7	1.8	2.2	2.3	2.2	1.9	0.9	0.9

4.2 Configuration and stage mass

To begin with, the Gross Lift-Off Masses (GLOM) of all analyzed configurations are shown in Fig. 12. The configurations are ordered by decreasing overall gross lift-off mass also making the distinction between reusable first stage and expendable upper stage.

It is remarkable that the hydrocarbon fuel configurations are by far the heaviest launchers. With a GLOM of 871 Mg and 815 Mg respectively, both the kerosene and the methane IAC configuration show lift-off masses of more than 800 Mg. In contrast, the hydrogen SC configurations using the IAC return option have a GLOM of around 330 Mg only. A relatively high GLOM from 401 to 529 Mg is found in the case of the configurations having reusable first stages employing the fly-back return method, with GLOM increasing significantly with first stage separation velocity. Gross lift-off masses below 400 Mg all belong to hydrogen IAC configurations. Here the GG configuration shows a GLOM of 389 Mg whereas the SC configurations using hydrogen as fuel and IAC as a return method have lift-off masses that are even approximately 15% lower.

The reusable first stage dry mass is shown in Fig. 13. Apart from showing the total dry mass of the RLV stage, Fig. 13 also displays the mass of the first stage rocket engines and its relative fraction within the total dry mass. The mass of rocket propulsion and its fraction play a role from the point of view of cost estimation since rocket engines represent a large portion of a reusable stage's value. Looking at the comparison of reusable first stage dry mass, the highest dry mass values going from 83 to 56 Mg are obtained by FB configurations. Methane and kerosene first stages have overall dry masses of 53 Mg and 49 Mg respectively with corresponding rocket engine mass fractions of 28% and 29.7% which are the highest among all considered configurations. While the hydrogen gas-generator configuration has a total dry mass of 45 Mg and an engine fraction of 16.6%, the hydrogen staged combustion configurations using In-Air-Capturing as the first stage return option have the lowest dry masses of 40 Mg to 34 Mg. The corresponding rocket engine fractions are 21% to 23.1% in this case. For the hydrogen staged combustion FB and IAC configurations with different first stage separation velocities, dry mass increases with separation velocity while the rocket engine fraction is slightly decreasing.

4.3 Reusable first stage reentry trajectories and loads

The calculation of reusable first stage reentry trajectories is an essential part of the presented analysis. In general, loads experienced by the reusable stage when reentering the atmosphere have a major influence on the technical feasibility of the transportation system and its potential economical

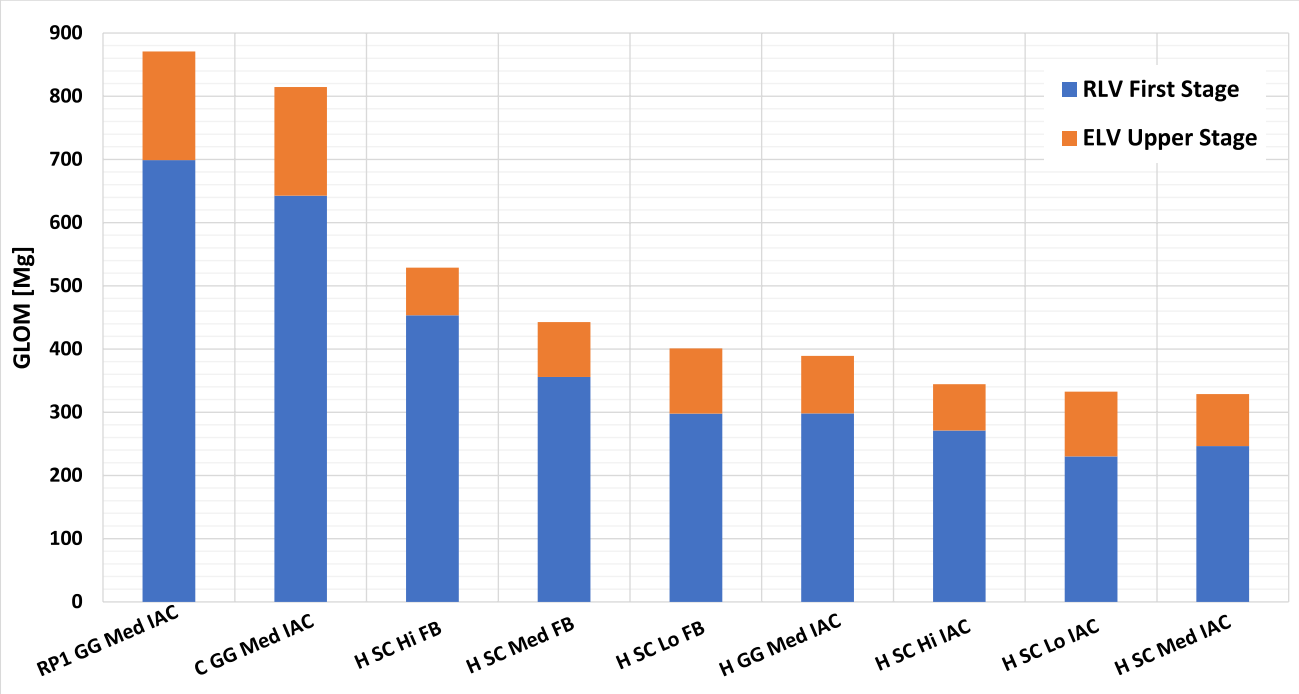

Fig. 12 Gross lift-off mass of analyzed VTHL configurations

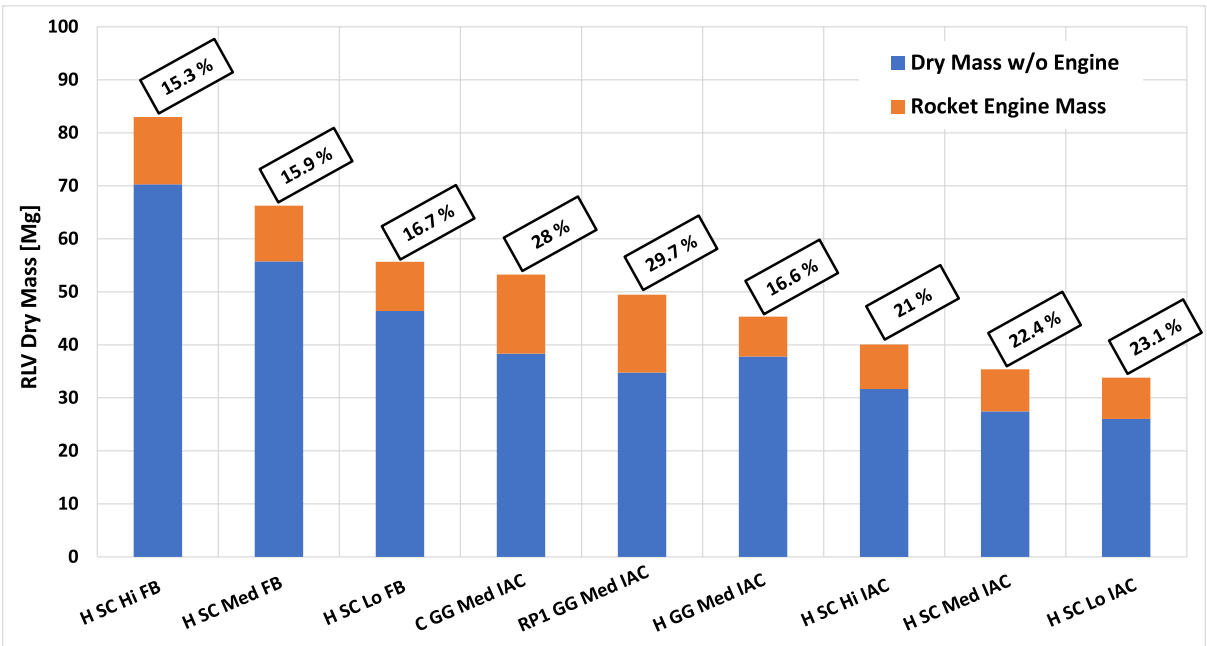

Fig. 13 RLV stage dry mass incl. rocket engine mass fraction

attractiveness. Keeping the loads low is thus imperative. In particular, the thermal protection system mass of all analyzed winged reusable first stages was determined based on reentry trajectory calculations and the related aerothermal loads present along the flight path. In addition, the fly-back fuel mass is a direct consequence of the distance to launch site resulting from the reentry trajectory calculation.

Reentry trajectory shape and loads are strongly dependent on the initial conditions at the beginning of the atmospheric reentry of the reusable first stage. Table 4 lists the

separation conditions, in particular velocity, altitude and flight path angle (FPA). The flight path angle at separation is positive and initially the reusable first stages continue to climb, however, after passing the apogee, approximately the same flight path angle magnitude is present when the stages begin to decelerate entering denser layers of the atmosphere. Thus, the flight path angle at separation has a strong influence on the reentry trajectory and the encountered mechanical and thermal loads. Therefore, for the ascent trajectories optimized for maximum payload in the target orbit also constraints for the pitch rate at launch are imposed. These constraints lead to reductions in flight path angle magnitude and only limited losses of payload performance. A threshold of 1 kPa for dynamic pressure at separation is respected as well to ensure a safe separation of the reusable first stages.

Table 4 Summary of RLV separation conditions

RLV Stage	Velocity [km/s]	Altitude [km]	FPA [deg]
H SC Hi FB	3.28	65.6	9.0
H SC Med FB	2.78	63.8	12.4
H SC Lo FB	2.27	60.1	17.5
H SC Hi IAC	3.16	67.4	10.5
H SC Med IAC	2.82	63.1	11.8
H SC Lo IAC	2.26	59.5	17.3
H GG Med IAC	2.67	64.6	17.5
C GG Med IAC	2.73	62.1	20.0
RP1 GG Med IAC	2.87	64.1	21.2

Reentry trajectories of all analyzed RLV stages are shown in Fig. 14 in terms of altitude as a function of Mach number. In this Mach-Altitude map the three different separation velocity classes are clearly identifiable. After first stage separation at altitudes between 60 and 67 km, the stages continue to climb reaching apogee altitudes up to 130 km, although in most of the cases the maximum altitude does not surpass 90 km.

When reaching denser layers of the atmosphere, the maximum stagnation point heat flux is reached at Mach numbers between 5.5 and 9.0 at altitudes between 30 and 50 km. The evolution of nose stagnation point heat flux along the reentry trajectory for all analyzed RLV stages is shown in Fig. 15 over the free-stream Mach number. Stagnation point heat flux is calculated using an empirical relation for a radius of 0.5 m which is the nose radius of the analyzed reusable first stages. Apart from the nose stagnation point heat flux, dynamic pressure and lateral load factor are also in the focus of the reentry trajectory analysis. For all reentry trajectories a limit of 4.0 is set for the lateral load factor n_z. Maximum values of n_z, dynamic pressure and stagnation point heat flux seen by the RLV stages during reentry are shown in Table 5.

Concerning dynamic pressure and heat flux the following is observed. Looking at the FB and IAC staged combustion configurations, one can see that with lower separation velocity maximum heat flux tends to decrease while the dynamic

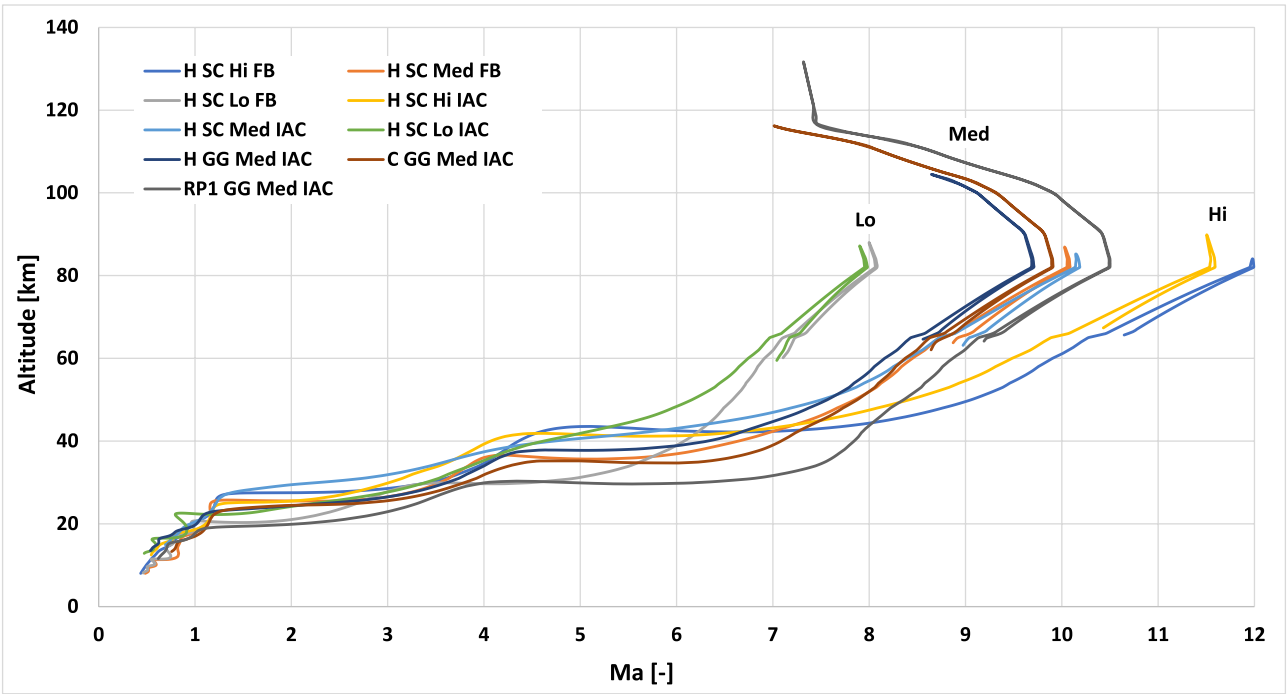

Fig. 14 Mach-altitude profiles of RLV stage reentry trajectories

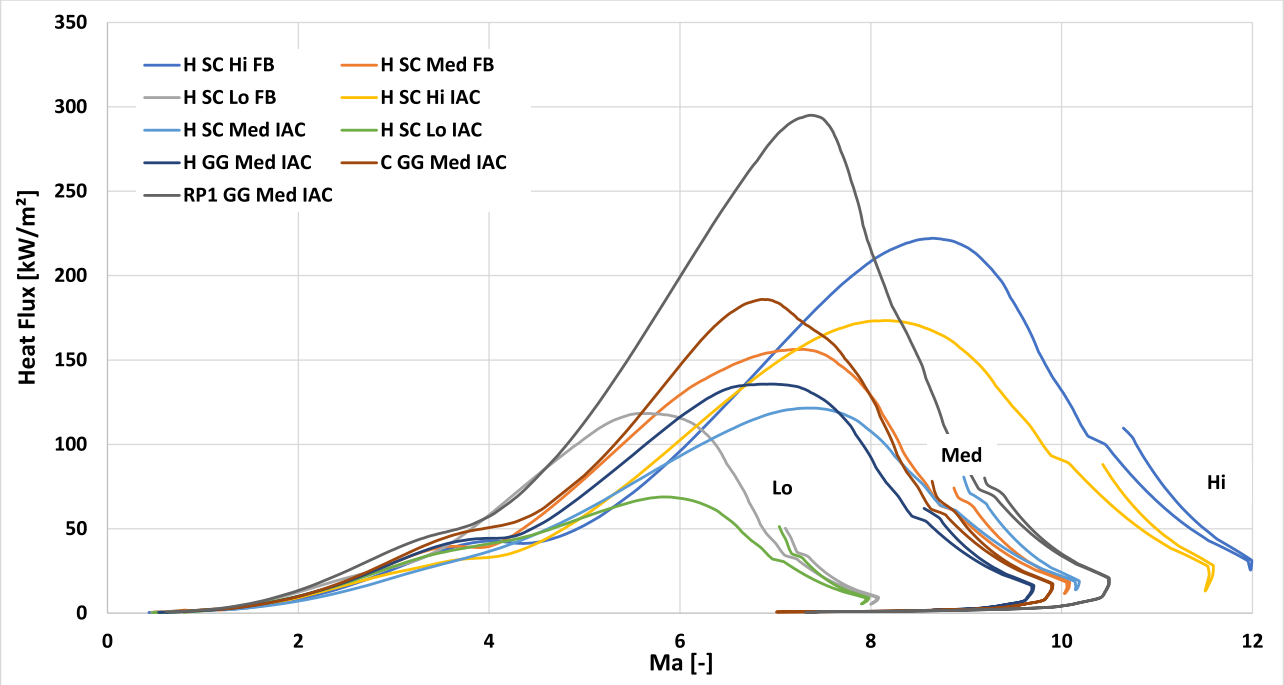

Fig. 15 Nose stagnation point Heat flux along RLV stage reentry trajectories

Table 5 Summary of maximum loads along reentry trajectories of RLV stages

RLV Stage	n_z [-]	P_{dyn} [kPa]	$\dot{q}$[kW/m^2]
H SC Hi FB	3.4	9.9	222
H SC Med FB	4.0	12.8	156
H SC Lo FB	4.0	17.8	118
H SC Hi IAC	3.9	8.4	173
H SC Med IAC	3.9	5.8	122
H SC Lo IAC	3.9	10.7	69
H GG Med IAC	4.1	12.9	136
C GG Med IAC	4.1	16.2	186
RP1 GG Med IAC	4.0	34	295

pressure tends to increase. The former is explained by the strong correlation between velocity and stagnation point heat flux. The latter is explained considering the flight path angle at separation, see Table 4. A strong increase of flight path angle magnitude is present with shorter first stage burn durations and lower separation velocities. This leads to steeper reentry trajectories and mostly higher peak dynamic pressures (proportionality to the square of velocity), while for the heat flux the influence of velocity is dominating (proportionality to the cube of velocity).

For the majority of the stages maximum heat flux and dynamic pressure stay below 200 kW/m^2 and 20 kPa respectively. However, in the case of the kerosene reusable first stage a maximum heat flux of 295 kW/m^2 and a dynamic pressure of 34 kPa are reached although its separation velocity class is medium. On the one hand, this is due to the high separation flight path angle of more than 21 deg (see Table 4) that leads to a steep reentry trajectory and a high apogee altitude (see Fig. 14). On the other hand, the ballistic coefficient of the kerosene stage is relatively high compared to the hydrogen first stages. Among the IAC stages the kerosene configuration has the most compact dimensions and at the same time the highest dry mass. This leads to a deep dive into the atmosphere and the observed relatively high maximum values of heat flux and dynamic pressure. An aerodynamic redesign might be considered in the future to improve this situation. It is important to note that in any case the preliminary RLV stage sizing is consistent as the encountered loads are used for the mass estimation of TPS.

5 Discussion of results

In this chapter, the results of the performed analysis are regarded from different points of view concentrating on a specific aspect of launch vehicle performance and/or reusable launch vehicle design. These aspects are the following: general performance characteristics of the transportation system, propellant combination and rocket propulsion efficiency, launch vehicle staging, winged reusable first stage return option and rocket engine cycle. This is done in line

with the formulated overall objective of this analysis that is to contribute to the identification of promising future European transportation systems.

5.1 Launch vehicle performance

The importance of the general launch vehicle performance might be considered secondary from a cost engineering point of view frequently brought up in connection with partially reusable space transportation systems. Apart from the complexity and the difficulties associated with cost estimation for partially reusable launch vehicles, this completely would neglect the fact that partially reusable systems need as well to be attractive from a performance point of view to become competitive. In general, reusability of any kind reduces the performance of a launch vehicle. Therefore, in the case of reusable systems the selection of high-performance design options has an even higher significance than in the case of expendable launch vehicles.

One way to compare different launch vehicle configurations is to focus on the ratio of the payload mass that is delivered to the target orbit and the lift-off mass of the transportation system. This so-called payload fraction is defined as:

$$\Pi = \frac{m_{P/L}}{m_{GLOM}} \tag{1}$$

For the configurations analyzed in this work the payload mass is fixed to 7.5 Mg ± 150 kg so that variations in payload fraction are completely due to variations in gross lift-off mass. However, the use of the dimensionless payload fraction is preferred since both payload mass and GLOM are reflected and even a comparison with other launch vehicles, that might have different payload masses and might serve different missions, would become possible.

The payload fraction of all analyzed configurations is shown in Fig. 16. First, there is a remarkable difference in payload fraction between the hydrocarbon configurations and the most performant hydrogen staged combustion variants. While the methane and kerosene configurations have payload fractions of 0.9% the maximum payload fraction achieved by the H SC Med IAC configuration is 2.3%, a factor of 2.6. Also noteworthy is the performance of the hydrogen staged combustion FB configurations, that are able to achieve payload fractions of 1.4% to 1.8% despite the disadvantages associated with this specific return option. It should be noted that among all analyzed configurations the FB stages are the only ones that are able to reach the launch site by their own means. While the hydrogen gas generator configuration achieves a payload fraction of 1.9%, the H SC IAC configurations show payload fractions of 2.2% to 2.3%. It is important to note the evolution of performance with separation velocity class. In case of the H SC IAC stages the highest performance is reached for the medium separation velocity class. This is in contrast to the evolution of payload fraction for the FB configurations, here a clear trend of growing performance with decreasing separation velocity of the reusable first stage exists. This is a clear reference to the staging optimum of the respective configuration type. In case of the H SC IAC configurations the optimum is covered

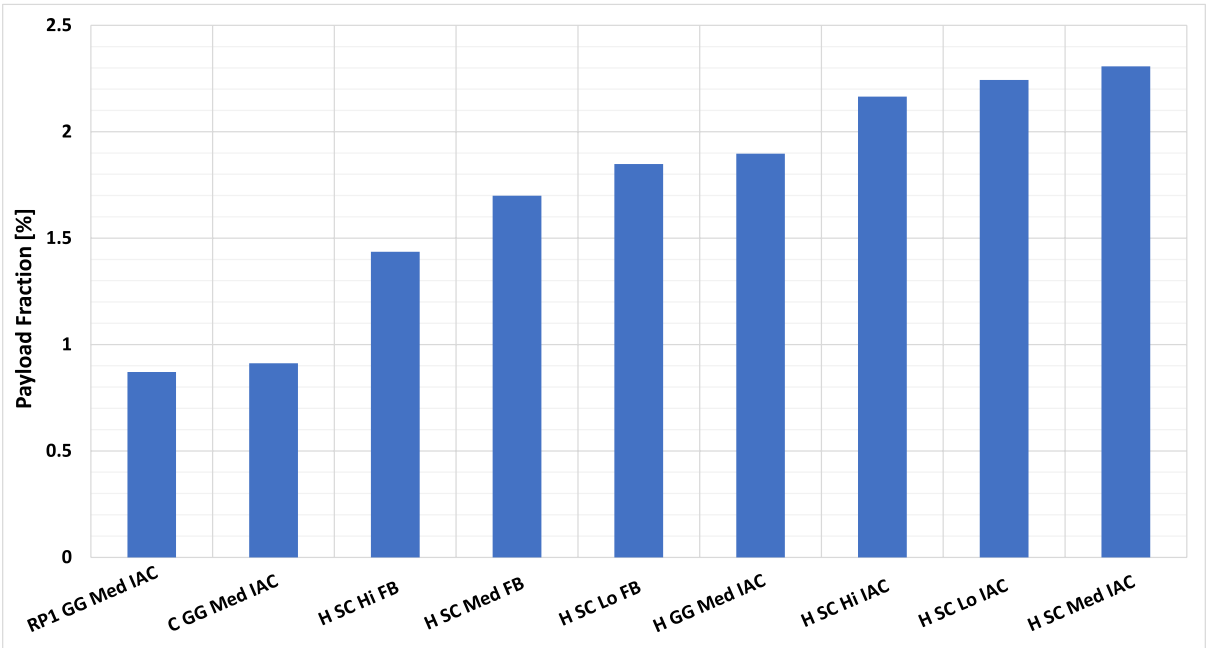

Fig. 16 Payload fraction of analyzed VTHL configurations

by the chosen separation velocity range, in case of H SC FB this is not the case.

Any attempt to explain the obtained overall launch vehicle performance expressed in terms of the payload fraction necessarily has to start with the well-known rocket equation:

$$\Delta v + \Delta v_{Loss} = c_e \ln m_i/m_f = c_e \ln R \quad (2)$$

The sum of the velocity change communicated to the launch vehicle and the delta velocity losses is equal to the product of the average specific impulse (expressed in the dimension of velocity) and the natural logarithm of the mass ratio. Mass ratio R is to be understood as the ratio of initial to final mass of the configuration.

While the significance of aspects like propulsion efficiency and staging is obvious, the gross delta velocity that needs to be delivered by the launch vehicle configuration stages and that includes the losses as well requires attention. The gross delta velocity including losses of all analyzed configurations is shown in Fig. 17. The bar chart shows the velocity changes actually performed by first and upper stages as well as the respective losses. The relevant losses are gravity, aerodynamic drag and thrust losses.

The defined nominal target orbit is a 1.5 km/s (remaining delta velocity to GEO) geostationary transfer orbit. The resulting gross delta velocity for the studied configurations is therefore between 11.2 km/s and 11.5 km/s. This variation is primarily due to different ascent trajectories and the associated losses. Small variations in the final orbit and payload mass have an additional, but minor effect. The delta velocity without losses, i.e. the actual velocity change, is between 9.8 km/s and 9.9 km/s. According to the defined and analyzed first stage separation velocity classes, the gross delta velocity of the reusable first stages is between 3.5 km/s and 4.6 km/s, including losses of 1.1 km/s to 1.3 km/s. Obviously, the biggest share of the delta velocity contribution is performed by the expendable upper stages. Their gross contribution is between 6.8 km/s and 7.9 km/s with relatively small losses of 240 m/s to 330 m/s. It is important to observe that, independent of the separation velocity class, the methane and kerosene configurations have the lowest first stage velocity losses of 1.1 km/s which is around 85% of the losses of the hydrogen configurations. This can be explained by the higher levels of thrust and mass flow of the hydrocarbon first stages as well as their relatively short burn time. In general, the first stage velocity losses are dominated by the gravity losses, while aerodynamic losses have a minor contribution. However, the effect of aerodynamic drag is reduced in the case of the hydrocarbon stages due to their still relatively high masses around the maximum of dynamic pressure during the ascent flight. Therefore, the fraction of aerodynamic losses is 9.4% to 11.1% for the hydrocarbon stages, whereas in the case of the hydrogen it is 14.5% to 14.9%.

5.2 Propellant combination and rocket propulsion efficiency

The effect of the choice of the propellant combination and the rocket propulsion efficiency on the outcomes of the presented work is apparent. However, a clear separation

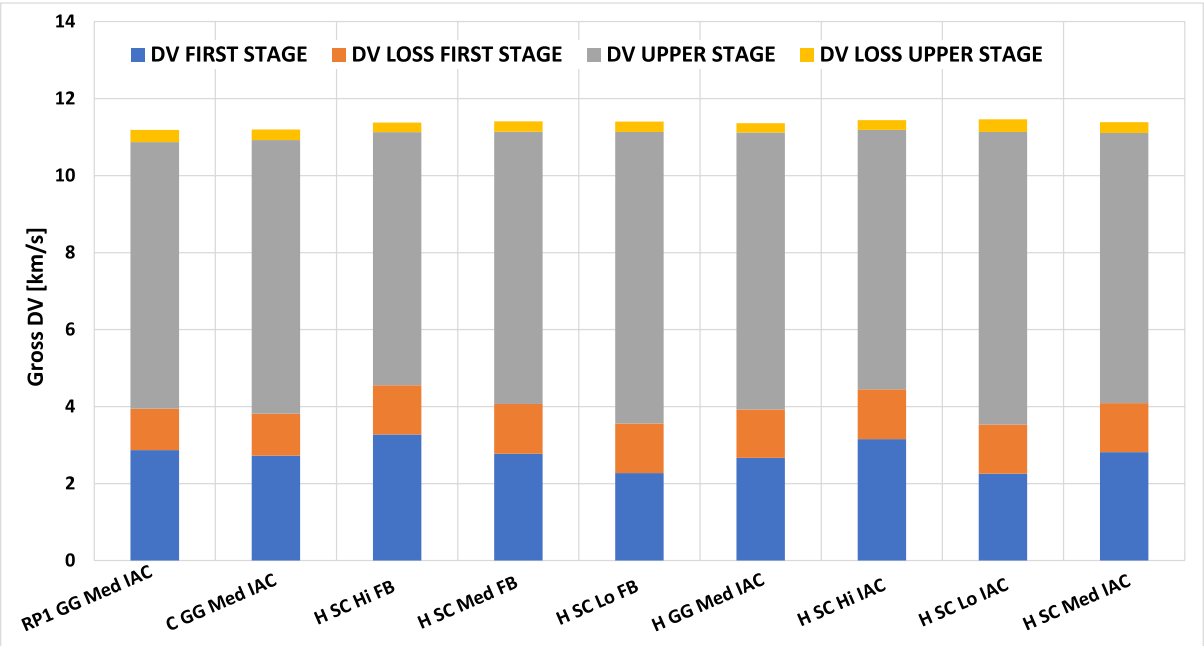

Fig. 17 Total gross delta velocity of analysed VTHL configurations during ascent

and isolation of this effect is not fully possible because the results for a certain configuration are under the influence of several, partially mutually dependent design aspects. In addition, due to limitations in the study scope not all details could have been analyzed. Thus, in the following mass results will be discussed for configurations having the same RLV stage return option and separation velocity class.

In Fig. 18 the specific impulse in dimensions of velocity is shown for the configurations having medium first stage separation velocity. Reusable first stage and expendable upper stage specific impulse is displayed. All shown variants use the IAC reusable first stage return method. The propellant combinations are RP1/LOX, LCH4/LOX and LH2/LOX. For hydrogen two rocket engine cycles, staged combustion and gas generator, are included, kerosene and methane configurations use the gas generator cycle only. The upper stage specific impulse is simply the vacuum specific impulse of the upper stage engines, whereas the shown first stage specific impulse is an effective specific impulse calculated with the rocket equation from velocity and mass data based on the optimized ascent trajectory. An overall specific impulse range from 3000 m/s to 4500 m/s is covered.

The lowest specific impulse values are those of the kerosene configuration with an upper stage Isp of 3310 m/s and a first stage effective Isp of 3020 m/s. The methane configurations' Isp is at 3420 m/s and 3120 m/s respectively. When going to hydrogen with gas generator cycle the efficiency significantly rises up to 4320 m/s for the upper and 3960 m/s for the reusable first stage. Efficiency in the case of hydrogen with staged combustion engines goes up even higher to values of 4500 m/s and 4190 m/s. Thus, hydrocarbon configurations have an Isp that is more than 25% lower than the Isp of the hydrogen stages. This is a significant drawback of hydrocarbon configurations in tendency leading to launchers with higher ascent propellant loadings and consequently also higher dry and overall lift-off masses.

A direct consequence of the reduced rocket propulsion efficiency is a necessary increase in mass ratio. The number of stages for the launchers analyzed in this study is limited to two and the only way to achieve similar delta velocities in the presence of a low Isp is to increase the mass ratio. This applies to both the reusable first stage as well as the expendable upper stage. The resulting final mass ratios at stage burnout for the reusable and expendable stages are shown in Fig. 19. While in the case of hydrogen staged combustion the mass ratios of the upper and first stage are 5.3 and 2.7 respectively, the kerosene configurations' upper stage needs a ratio of 9.2 and its first stage a ratio of 3.7 to perform the defined mission of bringing 7.5 Mg of payload to GTO. According to the rocket equation, the delta velocity depends on the natural logarithm of the mass ratio, see Eq. (2). Therefore, increases in mass ratio are less efficient for high values of R. However, due to the fixed number of stages low specific impulse necessarily requires higher mass ratios. This leads to the substantial GLOM increase observed for hydrocarbon configurations.

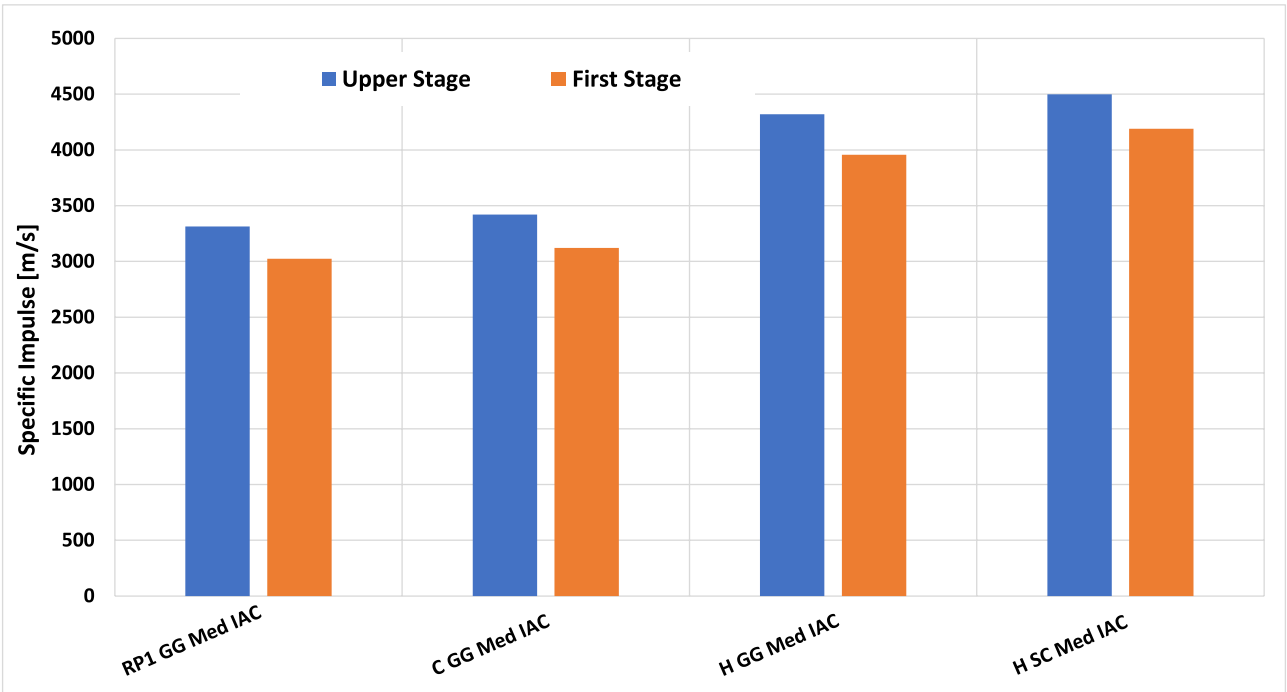

Fig. 18 Rocket propulsion efficiency for medium separation velocity variants

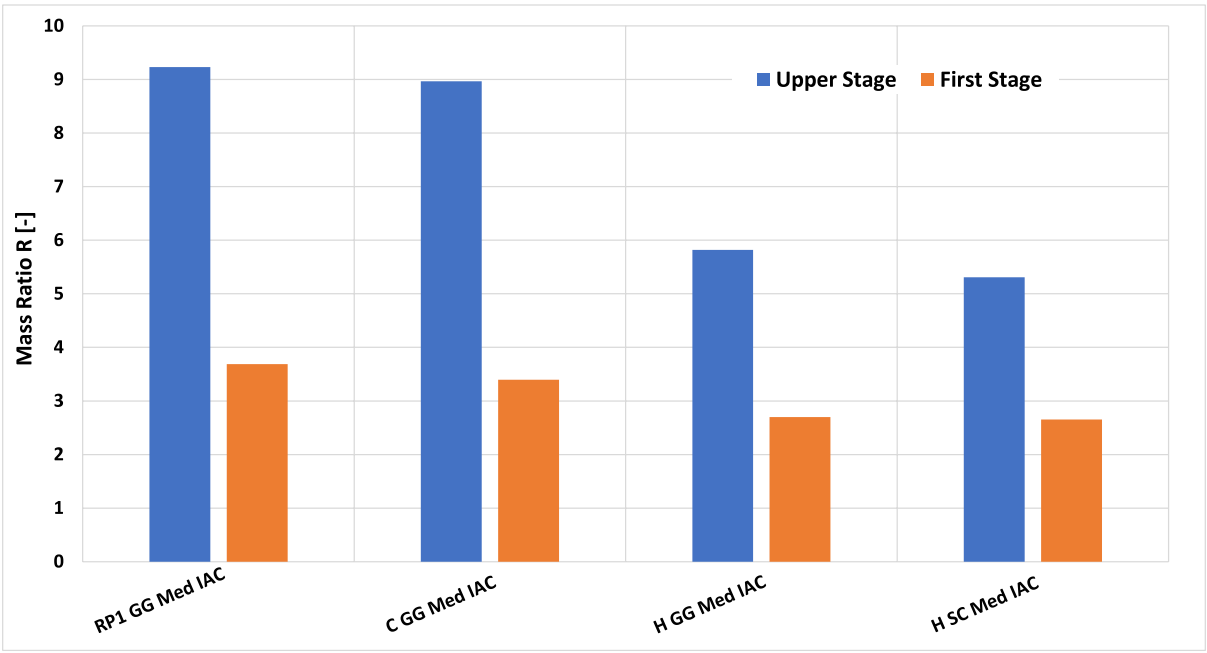

Fig. 19 Mass ratios for medium separation velocity variants

The non-dimensional GLOM for medium separation velocity IAC configurations is shown in Fig. 20 in reference to the maximum GLOM reached by the kerosene RLV. Since the propulsion efficiency of kerosene and methane is very similar, only a small difference in lift-off mass is observed. The methane configuration therefore shows a GLOM that is at 94% w.r.t. the reference. In contrast to that, the hydrogen gas generator configuration with Isp values of around 4000 m/s has a relative GLOM of just 45%. Finally, in the case of hydrogen staged combustion the advantages of the most efficient rocket propulsion lead to a relative GLOM of 38% as compared to the configuration using kerosene as fuel.

In addition to the comparison of GLOM, a comparison of reusable first stage dry mass is as well important due to the

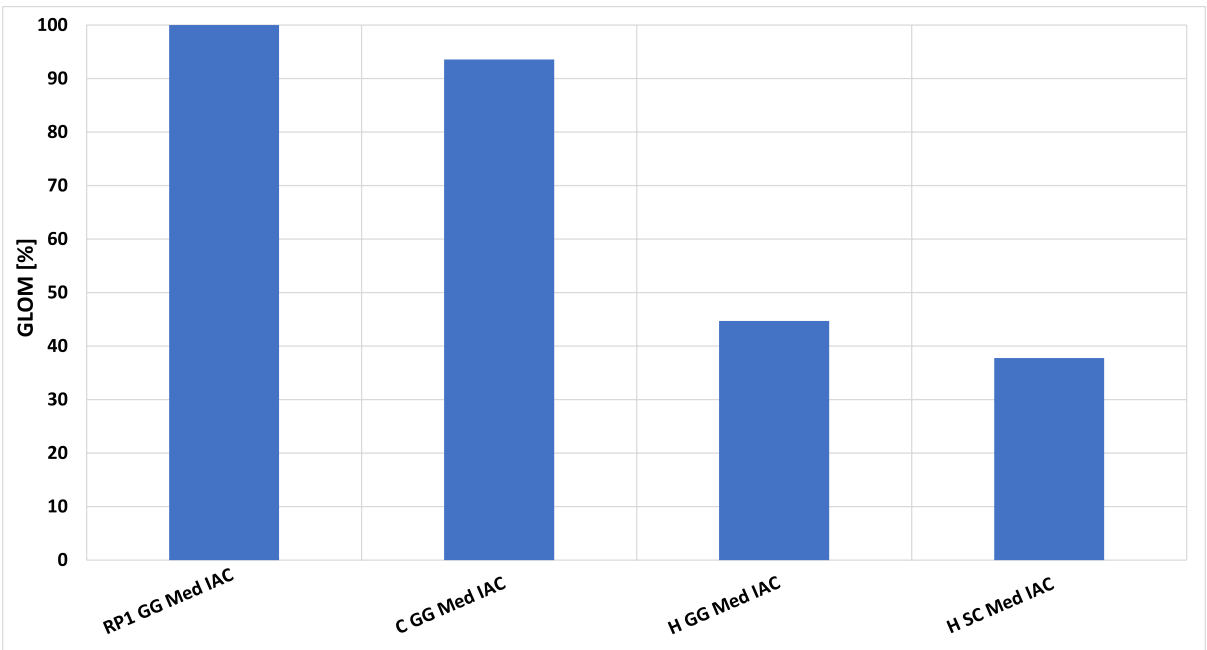

Fig. 20 Non-dimensional GLOM of medium separation velocity IAC configurations

significance of dry mass in the frame of cost estimations. A comparison of dry mass is shown in Fig. 21, a breakdown of dry mass in structural, subsystem, propulsion and thermal protection mass is shown. As in case of GLOM, hydrocarbon configurations again have the highest masses with the difference that methane has a dry mass slightly higher than kerosene. This is first of all because the structural mass in case of methane is higher as compared to kerosene. The Isp is higher by around 10 s in case of methane and thus the first stage ascent propellant loading is lower by approximately 60 Mg. However, the methane configurations fuel tank mass is higher by a factor of more than 1.5 due to its lower density relative to RP-1. As well remarkable is the fact that the hydrogen gas generator stage has a higher structural mass than the hydrocarbon variants. This is due to differences in stage length and diameter. Due to their higher diameters and shorter stage lengths (in addition to the higher fuel density as compared to hydrogen) the hydrocarbon RLV stages are less susceptible to bending and thus have relatively low structural masses. However, this is not enough to make up for their high propulsion system masses and the overall dry mass of hydrocarbons is still higher than the dry mass of the hydrogen gas generator stage. The reason for the very high propulsion system masses in the case of methane and kerosene is related to the requirement of an equivalent T/W ratio of 1.4 for all configurations. Thus, the low Isp of kerosene and methane leads to high GLOM which leads to a high thrust requirement which in turn leads to heavy rocket propulsion systems. While methane and kerosene have rocket engine fractions of 28% and 30%, in the case of the hydrogen stages the rocket engine fractions decrease down to 17% in the case of the gas generator cycle and down to 22% in the case of the staged combustion cycle. Due to its high specific impulse, the hydrogen staged combustion stage is still lowest both in overall dry mass as well as concerning the structural mass.

Finally, the important conclusion has to be drawn that in the frame of the defined constraints of the study at hand, not only do the hydrocarbon configurations have the highest GLOM, they as well show the highest RLV stage dry masses and the highest rocket engine fractions.

5.3 Launch vehicle staging

In general, two aspects are important in the context of launch vehicle staging, the number of stages and the distribution of propellant between the particular stages. The number of stages is a design choice usually made with the goal of using as few stages as possible. For the distribution of propellant between the stages a theoretical optimum leading to minimum lift-off mass and maximum payload fraction exists.

In the frame of the performed analysis, the number of stages is set to two for all analyzed configurations. The distribution of propellant between reusable und upper stages is oriented upon three separation velocity classes to obtain comparable separation conditions for the winged reusable stages. However, these predefined separation velocity classes do not necessarily correspond to an optimal distribution of propellant between the first and upper stage. This is illustrated by the comparison of GLOM for the configurations

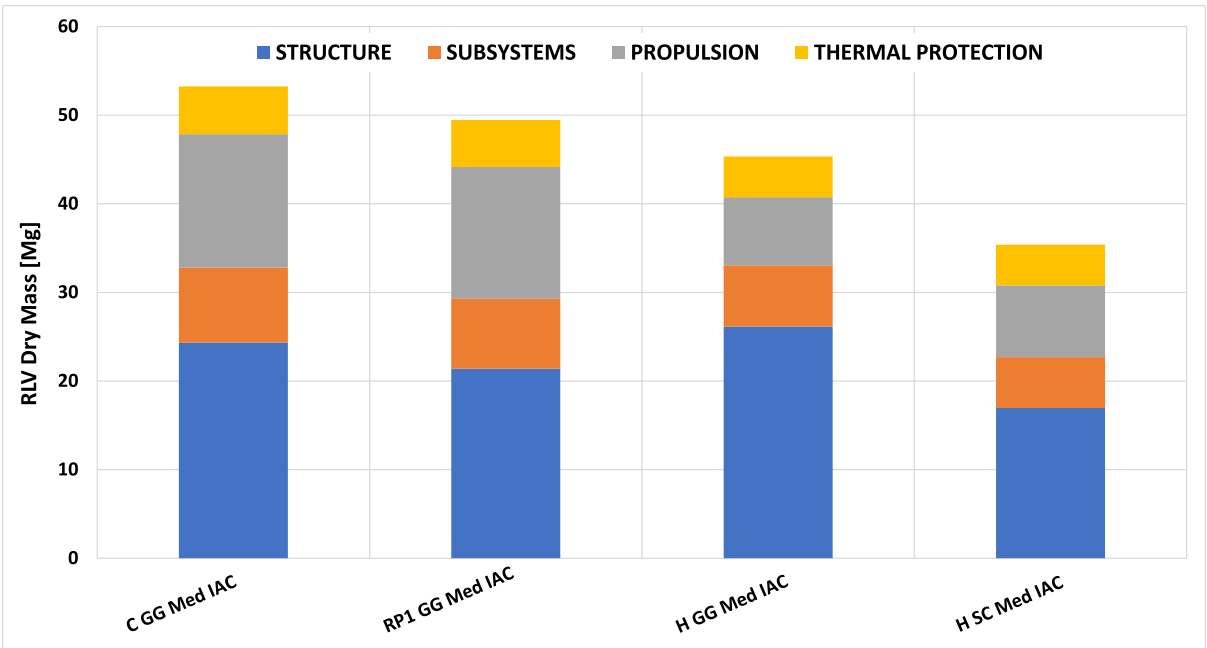

Fig. 21 Comparison of dry mass of medium separation velocity RLV (IAC) stages

using hydrogen as fuel and staged combustion as rocket engine cycle as shown above in Fig. 22.

All GLOM values are with respect to the GLOM of the Hi class FB configuration, which is 529 Mg. The Med IAC configuration shows a minimum in GLOM of 62%, although the difference as compared to Lo and Hi configurations with 63% and 65% is small. The fact that the GLOM of IAC configurations is almost insensitive to the separation velocity class is a standalone feature of this type of RLV. This is clearly not the case for the FB configurations. In case of FB there is a strong increase of GLOM instead. With the Lo and Med configurations having 76% and 84% GLOM respectively, an optimum cannot be seen within the chosen separation velocity range. The reason of the strong GLOM increase with first stage separation velocity is the fact that FB reusable stages contain additional hardware as air-breathing propulsion, a fly-back fuel tank and of course the fly-back fuel itself. The mass of this additional hardware and the fuel depend on the mass of the stage and the distance to launch site that needs to be flown using the air-breathing propulsion. Most likely, an optimum with regard to GLOM finds itself at a first stage separation velocity slightly below the Lo conditions, see Fig. 22. Thus, the comparison of configurations and stages with the same first stage separation velocity in certain cases does neglect the aspect of optimal staging. It is important to note, that the decision to focus on fixed staging points was taken in order to enable a faster design process in the frame of the general constraints of the performed analysis, see [1] and [4].

Concerning the number of stages for the analyzed configurations, an exactly defined point from which on a change to a three-stage configuration would be advantageous from a practical design point of view does not exist. However, the comparison of mass ratios shown in Fig. 19 suggests that at least for the hydrocarbon configurations an additional stage might be advantageous in terms of performance. This is important both from the point of view of performance as well as fuel comparison.

5.4 RLV Stage Return Option

In general, for the choice of the return option of a winged reusable first stage several aspects might be considered. Apart from the technical feasibility of the concept and its potential ability to serve defined mission scenarios, possible economic advantages related to the reusability of the first stage play an important role. But aspects like autonomy, flexibility and responsiveness also deserve consideration. Within this work only a preliminary, technical analysis for the return options Fly-Back and In-Air-Capturing is performed. For the return options FB and IAC analyzed in this work, three first stage separation velocities are considered. Depending on the first stage separation velocity and reentry mass of the stage, the descent of the reusable first stage results in different distances to launch site after the reentry. In Fig. 23 the RLV stage reentry mass is shown over the distance to launch site for the return methods FB and IAC. The resulting distances to launch site differ only slightly among FB and IAC as long as the separation velocity class remains the same. For the Lo separation velocity class the distance to the launch site is roughly 500 km, in the case of the Med class it is approximately 700 km and for the Hi class it is around 900 km. The reentry mass shown in Fig. 23 is the first stage dry mass plus the first stage residuals and reserves in the

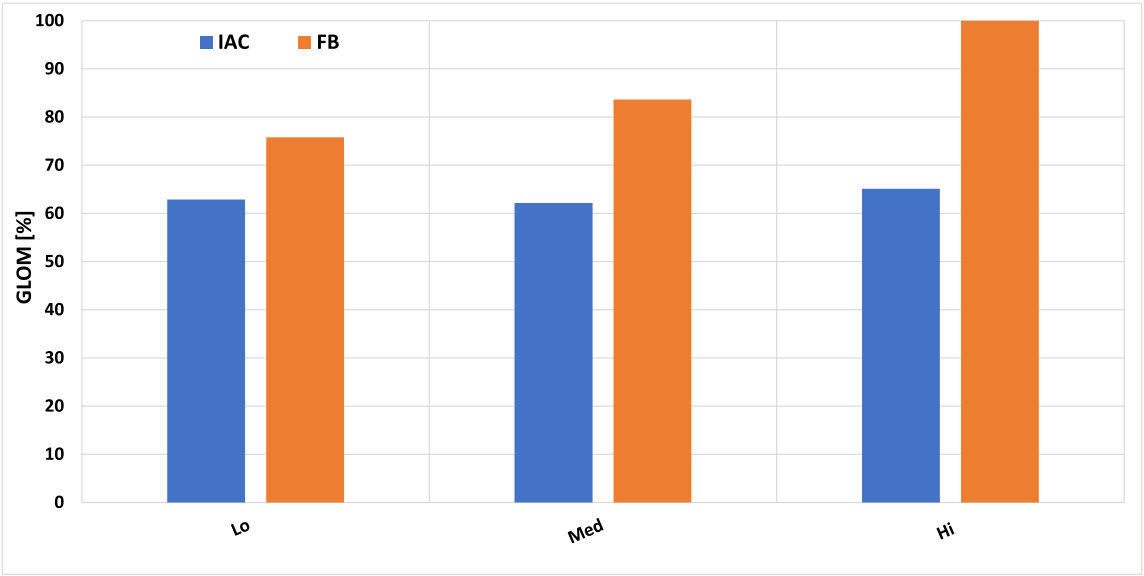

Fig. 22 Comparison in relative GLOM of hydrogen staged combustion configurations

case of IAC. For FB, the fly-back fuel mass is also part of the reentry mass. FB fuel masses of 4.5 Mg, 6.7 Mg and 11 Mg are required for the Lo, Med and Hi classes. Comparing the reentry mass, a similar trend as for the GLOM exists. In the case of FB a strong increase of reentry mass with first stage separation velocity is present, whereas for IAC only a weak correlation of reentry mass with first stage separation velocity is visible. In general, FB stages have significantly higher reentry masses than the IAC stages, e.g. for the Med class a factor of approximately two is observable, see Fig. 23 This is due to the additional hardware and fly-back fuel required in the case of FB as a return option. In Fig. 24 a comparison of the reentry mass for the Med IAC and Lo FB hydrogen staged combustion configurations is shown. The comparison of different separation velocity classes is justified because of the staging at or close to the optimum. In the case of FB, additional hardware and fuel are required. The FB hardware (FB H/W) consists of the FB fuel tank and the air-breathing propulsion. The FB hardware and fuel represent 11% and 7% of the total FB reentry mass, see Fig. 24

5.5 Rocket engine cycle

The effect of the choice of rocket engine cycle is primarily visible within a comparison of dry mass and rocket engine mass. The dry mass of the stage is to a certain extent an indicator for cost. However, the most valuable components of a launcher stage are its liquid rocket engines, so that mass units of dry mass are not enough for a cost estimation, the type of component representing a certain fraction of dry mass is important as well. Therefore, a comparison of RLV stage dry mass and its rocket engine mass and fraction is performed for the medium separation velocity class IAC hydrogen first stages to evaluate the effect of rocket engine cycle choice, see Fig. 25. The dry mass of the SC stage is around 35 Mg, whereas the GG stage has a dry mass about 10 Mg higher. The staged combustion cycle has the advantage of higher specific impulse. The disadvantage of staged combustion engines is their higher mass. The configurations analysed in this work are designed for a common T/W the launch of 1.4. However, the rocket engine mass of the SC stage is 7.9 Mg and thus higher as the rocket engine mass of the GG stage, which is 7.5 Mg only. This is the more remarkable as the GG configuration has a higher GLOM. The GLOM of the H SC Med IAC configuration is 329 Mg, whereas the H GG Med IAC has a GLOM of 389 Mg. This means, that despite a higher dry mass and a higher GLOM, the absolute mass of rocket engines is slightly lower for the GG reusable first stage. The reason for this is the higher rocket engine T/W of gas generator engines as compared to staged combustion engines. While the T/W of SC is around 75, in the case of GG the engine T/W goes up to 97, see [3] for more details. This also contributes to the differences in rocket engine fractions that can be observed for the SC and GG stages.

6 Summary and conclusions

In this work, nine partly reusable two-stage-to-orbit VTHL configurations with the mission of delivering 7.5 Mg to GTO are analyzed. The studied space transportation

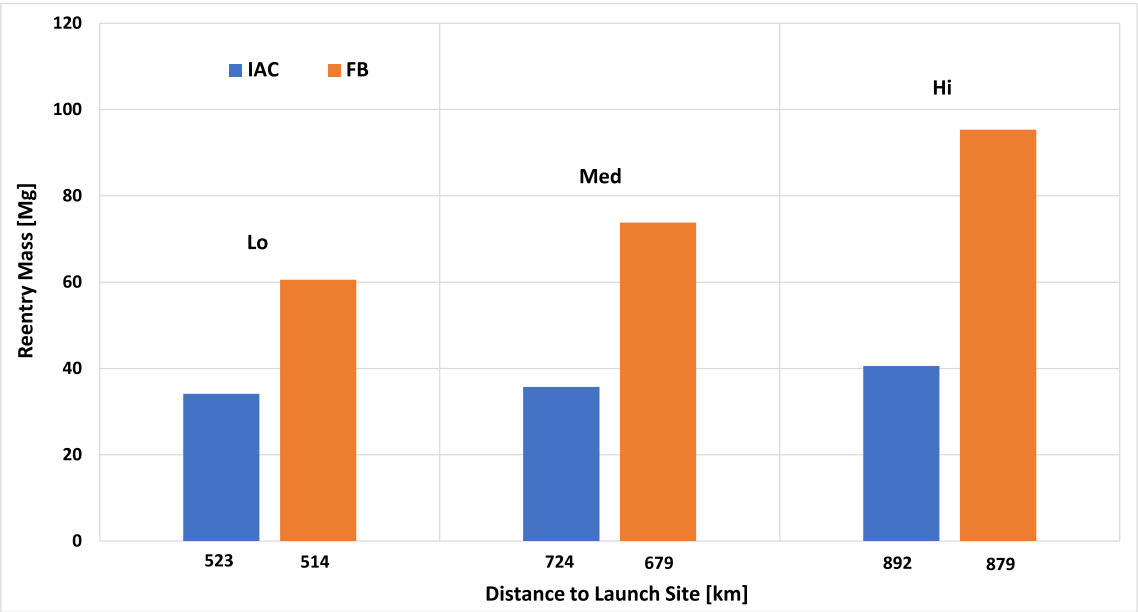

Fig. 23 RLV stage reentry mass and distance to launch site after reentry

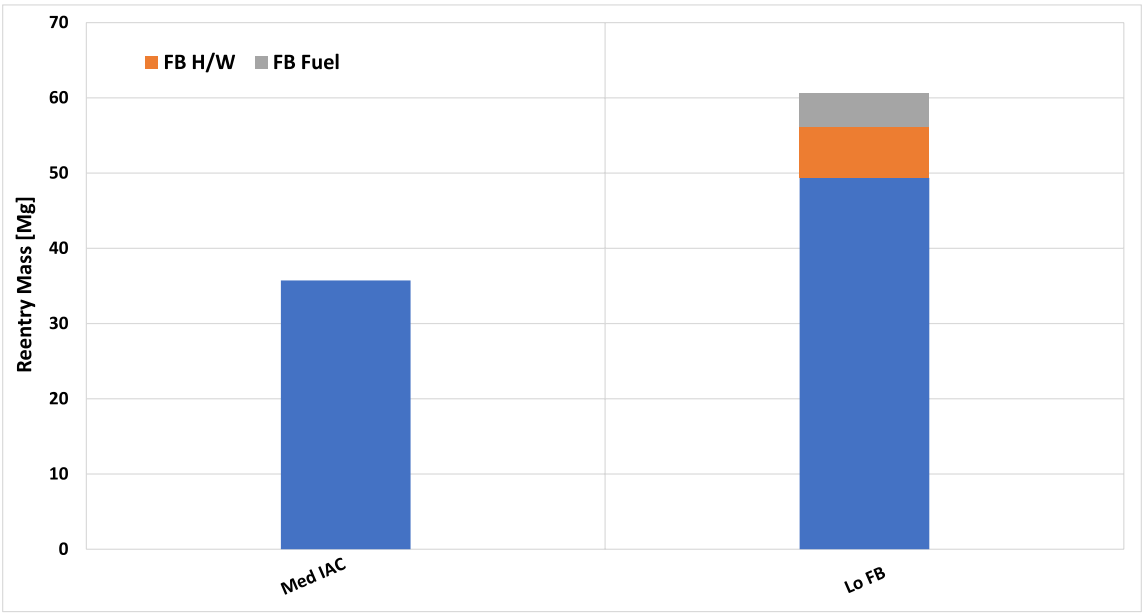

Fig. 24 Reentry mass comparison FB vs. IAC

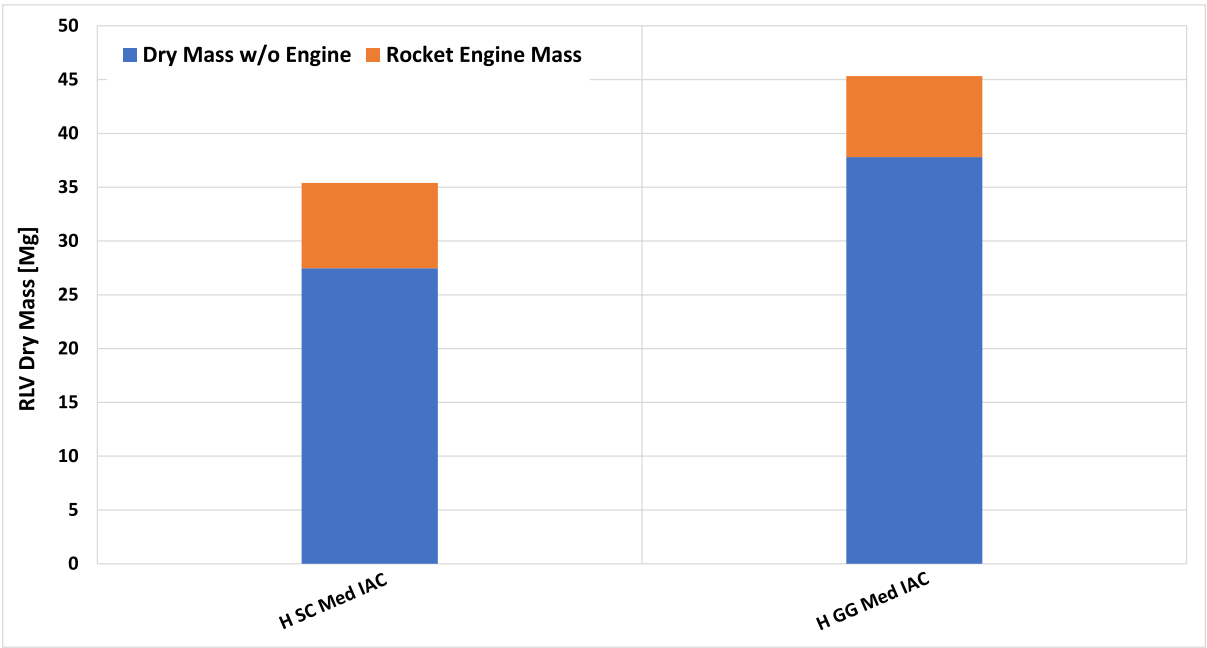

Fig. 25 Effect of rocket engine cycle on RLV stage dry mass

configurations consist of a winged reusable first stage and an expendable upper stage. The fuel/oxidizer combinations considered are LH2/LOX, LCH4/LOX and RP-1/LOX. Staged combustion and gas generator liquid rocket engine cycles are scaled in thrust within the iterative design process. Two return options for the winged reusable first stages, Fly-Back (FB) and In-Air-Capturing (IAC) are analyzed.

The following conclusions can be drawn from the presented results of the preliminary design of the studied RLV configurations: first, two-stage methane and kerosene configurations with winged reusable first stages do have GLOM higher by a factor of 2.1 as compared to hydrogen configurations. The reduction of payload fraction as compared to the most efficient hydrogen staged combustion configurations is as well by a factor of more than two. Furthermore, the

hydrocarbon stages not only have the highest GLOM but also the highest dry masses and rocket engine fractions. This is a consequence of the reduced specific impulse in case of methane and kerosene. Also, it is quantified to what extent FB as return option is depending on reusable first stage separation velocity. An increase of almost 60% in reentry mass is observed. In the case of IAC, only a very weak correlation between GLOM and separation velocity exists. The IAC hydrogen staged combustion configurations are the most performant in terms of GLOM and payload fraction. These stages cannot perform a return to launch site by their own means, thus performance-wise all IAC configurations need to be seen as downrange landing systems.

As an outlook, an interesting trade-off between performance and complexity (cost) could exist in the case of hydrogen gas generator configurations having relatively high payload fractions and low rocket engine masses.

Author contribution L.B. performed the preliminary analysis for VTHL systems within the presented study including all aspects of the design loop. I.D. substantially participated in the definition of the study logic, assumptions and constraints and prepared Fig. 1. M.S. calculated the rocket engines used as orientation in the entire study, defined the air-breathing propulsion characteristics. All authors reviewed the manuscript.

Funding Open Access funding enabled and organized by Projekt DEAL.

Data availability Not applicable.

Declarations

Conflict of interest The authors declare that there is no conflict of interest regarding the publication of this paper.

References

1. Dietlein, I., Bussler, L., Stappert, S., Wilken, J., Sippel, M.: Overview of system study on recovery methods for reusable first stages of future european launchers. CEAS Space Journal (2024). https://doi.org/10.1007/s12567-024-00557-9
2. Wilken, J., Stappert, S.: Comparative analysis of european vertical-landing reusable first stage concepts. CEAS Space Journal (2024). https://doi.org/10.1007/s12567-024-00549-9
3. Sippel, M., Wilken J.: Selection of Propulsion Characteristics for Systematic Assessment of Future European RLV-Options, CEAS Space Journal 2024. https://doi.org/10.1007/s12567-024-00564-w
4. Stappert, S., Dietlein, I., Wilken, J., Bussler, L., Sippel, M.: Options for Future European Reusable Booster Stages: Evaluation and Comparison of VTHL and VTVL Return Methods, CEAS Space Journal 2024. https://doi.org/10.1007/s12567-024-00571-x
5. Wilken, J., Herberhold, M., Sippel, M.: Options for Future European Reusable Booster Stages: Evaluation and Comparison of VTHL and VTVL Costs, CEAS Space Journal 2024. https://doi.org/10.1007/s12567-024-00577-5
6. Stappert, S., Singh, S., Funke, A., Sippel, M.: Developing an innovative and high-performance method for recovering reusable launcher stages: the in-air capturing method, CEAS Space Journal 2023
7. Guédron, S., Prel, Y., Bonnal, C., Rojo, I.: RLV concepts and experimental vehicle system studies: current status, IAC-03-V.6.05, 54th International Astronautical Congress, 2003
8. Baiocco, P.: Overview of reusable space systems with a look to technology aspects. Acta Astronaut. **189**(2021), 10–25 (2021)
9. Sippel, M., Manfletti, C., Burkhardt, H.: Long-term/strategic scenario for reusable booster stages. Acta Astronautica, Volume 58, Issue 4, February 2006.
10. Reusable Booster System: Review and Assessment, Aeronautics and Space Engineering Board, National Research Council, Washington D.C., 2012
11. Balesdent, M., et al.: Multidisciplinary design and optimization of winged architectures for resuable launch vehicles. Acta Astronaut. **211**, 97–115 (2023). https://doi.org/10.1016/j.actaastro.2023.05.041
12. Gogdet, O., Mansouri, J., Breteau, J., Patureau de Mirand, A., Louaas, E. 2019. Launch Vehicles System Studies in the Future Launchers Preparatory Programme: The Reusability Option for Ariane Evolutions. EUCASS https://doi.org/10.13009/EUCASS2019-971
13. Kayal, H.: Aufbau eines Vereinfachten Simulationsmodells für den Bahnaufstieg in der Großkreisebene, DLR-IB 318–93/05
14. Picone, J. M., et al.: NRLMSISE-00 empirical model of the atmosphere: Statistical comparisons and scientific issues. Journal of Geophysical Research: Space Physics 107.A12 (2002): SIA-15
15. Klevanski, J., Sippel, M.: Quasi-Optimal Control for the Reentry and Return Flight of an RLV. 5th International Conference on Launcher Technology, Madrid 2003
16. Klevanski, J., Sippel, M.: Beschreibung des Programms zur Aerodynamischen Voranalyse CAC Version 2, DLR IB 647–2003/04, SART TN-004 / 2003, DLR Cologne 2003
17. Finck, R.D.: USAF Stability and Control DATCOM, AFWAL-TR-83–3048
18. Reisch, U., Streit, T.: Surface Inclination and Heat Transfer Methods for Reacting Hypersonic Flow in Thermochemical Equilibrium, DLR IB 129–96/10, Braunschweig 1996
19. Myers, D.E. et al.: Parametric Weight Comparison of Advanced Metallic, Ceramic Tile and Ceramic Blanket Thermal Protection Systems. NASA TM-2000–210289
20. Waldmann, H., Sippel, M.: Adaptation Requirements of the EJ200 as a Dry Hydrogen Fly Back Engine in a Reusable Launcher Stage. ISABE-2005–1121, September 2005